Functional Analysis of Phosphoinositides and Their Effectors Involved in Trogocytosis and Phagocytosis in *Entamoeba histolytic*a

A Dissertation Submitted to
The Graduate School of Life and Environmental Sciences,
The University of Tsukuba
in Partial Fulfillment of the Requirements
for the Degree of Doctor of Philosophy in Science
(Doctoral Program in Biological Sciences)

Natsuki WATANABE

Table of Contents

Abstract

Entamoeba histolytica is an enteric protozoan parasite which inhabits the human intestine and liver. It is the causative agent of amoebasis, a disease that affects 50 million patients, mostly from developing countries, and causes 100,000 deaths per year worldwide. Disease transmission is via ingestion of fecally-contaminated food and water. However, in developed countries such as Japan, reported cases are either acquired from traveling abroad or through sexual contact. There are over 1,000 reports per year in Japan and the infection rate shows an increasing tendency annually, making amoebiasis one of the most important protozoan infectious diseases in the country.

E. histolytica inflicts damage to its host through pathogenic mechanisms that include two modes of cell uptake: phagocytosis and trogocytosis. Phagocytosis is a process in which *E. histolytica* takes dead mammalian cells as a whole. Previously, it was reported that phagocytic activity-deficient mutant demonstrated reduced pathogenic efficiency. On the other hand, the process in which *E. histolytica* nibbles living cells and bites distinct pieces of cells is called trogocytosis. Amoebic trogocytosis ultimately results in the death of nibbled mammalian cell. Both phagocytosis and trogocytosis in amoeba are completely distinct processes as reflected by the differences in their mechanisms for target cell recognition, invagination with cytoskeletal reorganization, and target cell fate. Compared with model organisms, only some of the molecules involved in these processes are conserved in *E. histolytica*, suggesting that there are lineage- or species-specific pathways facilitated by functional analogues. The objective of this research is to clarify the mechanisms of phagocytosis and trogocytosis in *E. histolytica*. It leads to a deeper understanding of conserved, as well as divergent fundamental mechanisms among eukaryotes.

In this research, the focus is on phosphatidylinositol phosphates (PIPs) which are phospholipids that are well-conserved in eukaryotes. There are seven isotypes based on the phosphorylation state at the D3, D4, and D5 position of the inositol ring. Seven different types of

PIPs work as spatiotemporal-specific signal to recruit specific binding proteins against each seven PIPs. They are key molecules to regulate multifarious mechanisms involved in cytoskeletal reorganization, signal cascade pathways, and vesicular trafficking. In macrophage, it is known that $PI(4,5)PI_2$ and $PI(3,4,5)P_3$ are important for actin reorganization during phagosome formation, while PI3P is important for phagosome maturation and lysosome fusion after phagosome closure. In *E. histolytica*, it is clear that there are three kinds of PIPs, PI3P, $PI(4,5)P_2$, and $PI(3,4,5)P_3$, and they showed similar localization as other organisms. In addition, PI3P is localized not only on phagosomes but also on trogosomes, as visualized using FYVE (Fab1, YOTB1, Vac1, EEA1) domain, a PI3P biosensor. However, PIPs metabolisms, transportation, and distribution are not clear in *E. histolytica*. PIPs binding molecules are not well conserved and PIPs downstream effector is unknown.

To obtain an overview of PIPs metabolisms, I searched for PIPs metabolic enzymes from *E. histolytica* genome using nineteen human PI-kinases and twenty-five human phosphatases as queries. As a result, ten PI-kinase candidates and thirty-four PI-phosphatase candidates were identified in *E. histolytica*. However, a few subclasses of these enzymes lack homologues in *E. histolytica*. Despite this, all PIPs could be synthesized and metabolized by the bypass pathway. Interestingly, the enzymes related to metabolisms of $PI(3,4,5)P_3$ are divergent. It shows the importance of $PI(3,4,5)P_3$ as second messenger. Specifically, I focused on PI3-kinases and PI3-phosphatases which respectively phosphorylate and dephosphorylate the D3 position of the inositol ring because of their diversity.

To clarify PIPs signal molecules and mechanisms during phago/trogocytosis, I identified PI3P binding molecules localized on phagosome in *E. histolytica*. To specifically identify the molecules which bind to PI3P during phagocytosis, GFP tagged FYVE domain-expressing *E. histolytica* transformant under tetracycline-induced condition was established. PI3P downstream molecules cannot bind to PI3P because GFP-FYVE blocked PI3P by the specific binding ability of

the FYVE domain. The phagosome proteome results between GFP-FYVE expressing cells and non-expressing cells were compared. Ninety-four proteins were identified as PI3P downstream molecule candidates in the phagosome proteome from this new PI3P blocking method. The retromer complex components, vacuolar protein sorting 26 (Vps26) and Vps35, were found with more than two times higher against PI3P blocked phagosome fraction. The retromer complex is an adaptor which regulates retrograde transport of lysosome hydrolase receptors from endosome to Golgi. In humans, the retromer complex is composed of Vps26/29/35, known as the cargo recognition complex, and two kinds of sorting nexin (SNX), SNX1/2 and SNX3. Both SNX1 and SNX2 have PX domain, which is known as a PI3P binding domain, and BAR domain, which is involved in membrane curvature, whereas SNX3 only contains a PX domain. The retromer complex is recruited on the membrane through PI3P binding by the PX domain of SNX3. As EhVps26 and EhVps35 could not bind to PI3P, I searched for EhSNX homologue(s) using human SNX1 sequence as a query, since it is plausible that these EhVps bind to PI3P via EhSNX homologue(s). As a result, two EhSNX (EhSNX1 and EhSNX2) were found. They have similar structure with human SNX3 as they only contain the PX domain. EhSNX1 and EhSNX2 specifically bound to PI3P, whereas EhSNX1 localized on trogocytic cup during trogosome formation, and EhSNX2 localized on phagosome after phagosome closure as observed by lipid overlay assay and immunofluorescence assay respectively. Moreover, I confirmed that EhSNX1, but not EhSNX2 binds with EhVps26 by immunoprecipitation using anti-Vps26 antibody. The phago/trogocytosis efficiencies were upregulated by *EhSNX2* gene silencing, suggesting EhSNX2 is involved in the negative regulation of phago/trogocytosis. These results show that PI3P signaling is important for phago/trogocytosis in *E. histolytica* and that EhSNX1 and EhSNX2 are recruited to phago/trogosomes spatiotemporally. Also, the results suggest that EhVps26 and EhVps35 were recruited to phagosomes via EhSNX1. In *E. histolytica,* twelve FYVE domain containing proteins (EhFP1-12) were found as PI3P-binding protein candidates by a previous study,

but all of them did not bind to PI3P. In this study, I have identified PI3P binding proteins and clarified their importance. Finally, this research also shed light on specific parts of the mechanisms of phago/trogocytosis in *E. histolytica*.

Chapter 1. General Introduction

1-1 Phosphatidylinositol

Phosphatidylinositol phosphates (PIPs) are derivatives of PIs and play pivotal roles in a variety of biological processes such as receptor-mediated signaling, vesicular traffic, cytoskeleton rearrangement, and regulation of channels and transporters (Sasaki *et al*., 2009; Balla, 2013). Spatiotemporal regulation of PI-mediated biological processes is achieved by interconversion of the phosphorylation states of PIs by specific kinases and phosphatases, followed by recruitment of PI-specific effectors.

PI is one class of glycerophospholipids that is composed of an inositol ring, a phosphate, a glycerol skeleton, and two acyl chains. PI converts to seven types of PIPs by PI-kinases and PI-phosphatases: three types of PIP, three types of PIP_2, and one PIP_3 (Fig. 1). These seven different types of PIPs are localized on different cellular compartments and mediate a variety of the intracellular events by recruiting proteins possessing PIPs-recognizing domains such as FYVE (Fab1, YOTB1, Vac1, EEA1), pleckstrin-homology (PH), and phox homology (PX) domains.

These seven isotypes of PIPs are ubiquitously distributed on the membrane of the cell or vacuoles. Some PIPs have important roles during phagosome formation and development in mammalian cells. PI(4,5)P2 is needed in forming the phagocytic cup, PI(3,4,5)P3 is involved in the sealing of phagosomes, and PI3P is required during the internalization and maturation of phagosomes.

1-2 PI3-kinases and PI3-phosphatases

PI3-kinases phosphorylate the hydroxyl group at the D3 position of the inositol ring of PI, PI, PI4P, and $PI(4,5)P_2$ to generate PI3P, $PI(3,4)P_2$, and $PI(3,4,5)P_3$, respectively. There are three subfamilies of PI3-kinases: class I, II, and III (Sasaki *et al*., 2009). In general, class I enzymes preferentially generate $PI(3,4,5)P_3$ from $PI(4,5)P_2$. Class II enzymes mostly generate $PI(3,4)P_2$ from

PI4P and also generate PI3P from PI. Class III enzymes almost exclusively generate PI3P from PI. In mammals, there are 8 members of PI3-kinases. All PI3-kinases contain a "signature motif" consisting of the catalytic kinase domain, a helical domain, also called "lipid kinase unique (LKU) domain," and a membrane-binding C2 domain (Marat & Haucke, 2016; Vanhaesebroeck *et al*., 2010; Balla, 2013).

PI3-phosphatases are categorized into two groups based on substrate specificities. One group includes phosphatase and tensin homologue deleted on chromosome ten (PTEN) and TPIP (TPTE and PTEN homologous inositol lipid phosphatase), while the other group includes myotubularins (MTMs). PTEN and TPIP have similar catalytic domains but differ in substrate specificity. PTEN removes the phosphate moiety at the D3 position of PI(3,4,5)P_3 and PI(3,4)P_2, while TPIPs dephosphorylate any of the 3′-phosphorylated inositides at the D3 position (Walker *et al*., 2001; Malek *et al*., 2017). On the other hand, MTMs remove the D3 phosphate from PI(3,5)P_2 and PI3P. The catalytic center of both groups of PI3-phosphatases contains the CX_5R motif, which is also found in protein tyrosine phosphatases (Hsu & Mao, 2015).

1-2 The retromer complex components and their role

The retromer complex is composed of the cargo-selective complex, Vps26/29/35, and two kinds of sorting nexin (SNX), SNX1/2 and SNX3. The retromer complex mediates retrograde transport from endosome to the Golgi apparatus. Vacuolar protein sorting 10 (Vps10) and cation independent mannose 6-phosphate receptor (CI-M6PR) are well known cargoes of the retromer. The retromer subunits, especially the members of the cargo-selective complex, are well conserved among many organisms from yeast to mammals. The retromer makes a stable complex of Vps26/29/35, but also forms a more transient association with SNX components (Swarbrick *et al*., 2011). For cargo selection, the cargo-selective complex should be recruited to the membrane. It is known that SNX3

(containing only the PX domain) recruits the retromer to the membrane through its PX domain to bind PI3P on the surface. The binding of SNX3, Vps26, and Vps35 occurs via the N-terminal and PX domain of SNX3, and the C-terminal of Vps26, and the N-terminal of Vps35 (Lucas *et al*., 2016).

1-3 Intestinal protozoan parasite *Entamoeba histolytica*

Entamoeba histolytica is an enteric protozoan parasite which inhabits the human intestine and liver. It is the causative agent of amoebasis, a disease that affects 50 million patients, mostly from developing countries, and causes 100,000 deaths per year worldwide. Disease transmission is via ingestion of fecally-contaminated food and water. However, in developed countries such as Japan, reported cases are either acquired from traveling abroad or through sexual contact. There are over 1,000 reports per year in Japan and the infection rate shows an increasing tendency annually, making amoebiasis one of the most important protozoan infectious diseases in the country. Pathogenesis of amoebiasis requires the invasion of intestinal epithelial tissues or extraintestinal tissues via blood vessels by the amoeba trophozoites. *E. histolytica* displays inherited capacity of ingestion of foreign cells by phagocytosis and trogocytosis (Ralston *et al*., 2014). Amoeba ingests whole cell by phagocytosis and bites off and ingests distinct host cell fragments by trogocytosis.

It has been confirmed that PI3P is localized on the trogocytic cup and the trogosome during CHO cell trogocytosis based on fluorescence imaging using trophozoites that overexpress GFP-FYVE (Nakada-Tsukui *et al*., 2009). This suggests that PI3P is involved in trogocytosis. In addition, PI3P effectors also play a role in general endocytosis or phagocytosis, however the homologues of PI3P effectors are not conserved in *E. histolytica*. A previous *in silico* BLAST search of the *E. histolytica* genome was conducted to find FYVE-domain containing proteins (EhFPs) which may bind to PI3P. Surprisingly, all of the HA-tagged EhFPs that were expressed in *E. histolytica* did not bind to PI3P. Thus, it is remains imperative to find out the PI3P effector in order to improve our

understanding of the mechanisms of amoebic trogo/phagocytosis.

Chapter 2. Functional analysis of phosphoinositides and their effectors involved in trogocytosis and phagocytosis in *E. histolytica*

2-1 Materials and Methods

2-1-1 *In silico* search for PI3-kinases homologues in *E. histolytica*

BLAST search was done by probing the *E. histolytica* HM-1:IMSS genome in the AmoebaDB genome database (http://amoebadb.org/amoeba/), using human class I PI3-kinases (NP_006209, NP_006210, AAH35683, and NP_005017, corresponding to p110α, β, γ, and δ, respectively) as queries. A BLAST search for Class II PI3-kinases was performed using human class II PI3-kinases, NP_002636, NP_002637, and NP_001275701, as queries. Likewise, class III PI3-kinases were searched using AAH53651 as a query. Human Vps15 (NP_055417) was also used as a query for searching class III PI3-kinase regulatory subunit.

2-1-2 *In silico* search for PI3-phosphatases homologues in *E. histolytica*

To search for *E. histolytica* homologues of PI3-phosphatases, I used the lone human PTEN protein (AAD13528) as query for BLAST search. On the other hand, the other human PI3-phosphatases such as myotubularins (MTM) and MTM related proteins (MTMR) have many members, which are categorized into groups based on their domain structure and organization. So, MTMR1 (NP_000243), MTMR3 (AAI52456.1), MTMR6 (EAX08367.1), MTMR9 (NP_056273.2), MTMR14 (AAH01674.2), MTMR15 (NP_002963.2) were used as representative MTMR query sequences.

2-1-3 Cells and reagents

Trophozoites of *E. histolytica* strains HM-1:IMSS cl6 (Diamond *et al*., 1972) and G3 (Bracha *et al*., 2003) were axenically cultured in BI-S-33 medium (BIS) at 35.5ºC as previously

described (Diamond *et al*., 1978). Chinese hamster ovary (CHO) cells were maintained in F-12 medium (Invitrogen-Gibco, Grand Island, NY) supplemented with 10% fet al bovine serum in 25 cm^2 tissue culture flasks (IWAKI, Shizuoka, Japan) under 5% CO_2 at 37ºC. All chemicals of analytical grade were purchased from Sigma Aldrich (Missouri, USA) unless otherwise stated. The anti-HA (11MO) and anti-myc (9E10) monoclonal antibodies were purchased from Covance (Princeton, NJ, USA). The anti-GFP antibody was purchased from Sigma Aldrich. The production of rabbit polyclonal antibodies against EhCS1, EhCP-A5, EhVps26, and EhVps35 were previously described (Nozaki *et al*., 1999; Nakada-tsukui *et al*., 2005; Nakada-Tsukui *et al*., 2009).

2-1-4 Plasmid construction

Standard techniques were used for DNA manipulation, subcloning, and plasmid construction. Plasmid vectors to produce *E. histolytica* lines that express EhSNX1 (EHI_060320) and EhSNX2 (EHI_004400) with HA- or GFP-tag fused at the amino and carboxyl termini were constructed as follows. The full-length protein coding region of these genes was amplified by PCR with the following primer pairs; 5’-GAACCCGGGATGGGAGATAATAAAGAAGATATTAT -3’ and 5’- GAACTCGAGTTATTCTGATGATGATGAACTTTCAT -3’ (*EhSNX1*) or 5’-GAACCCGGGATGAGTAATTATGCACAGTATGAATA -3’ and 5’-GAACTCGAGTTACCAACTAGTAACTTCCCAATTGT -3’ (*EhSNX2*), where the restriction enzyme sites are underlined. PCR-amplified fragments were digested by *Xma*I (NEBiolabs, Massachusetts, USA) and *Xho*I, and ligated with DNA ligation kit (TaKaRa Bio, Shiga, Japan) into similarly digested vectors, pEhEx-HA (haemagglutinin) (Yousuf *et al*., 2010) and pEhEx-GFP vectors (green fluorescent protein) (Somlata, Nakada-Tsukui, & Nozaki, 2017), to produce HA-tagged and GFP-fused SNXs at the amino terminus. The resultant plasmids were designated as pEhExHA-SNX1, pEhExHA-SNX2, pEhExGFP-SNX1, and pEhExGFP-SNX12, respectively.

Note that pEhExGFP contains a linker corresponding to 5 repeats of GA dipeptides after the full length GFP amino acid sequence. To construct plasmids to express EhSNX1 and EhSNX2 with HA tag at the carboxyl terminus, the full-length protein coding sequence of these genes was amplified by PCR with the following primer pairs: 5'-GAAAGATCTATGGGAGATAATAAAGAAGATATTAT -3' and 5'-GAAAGATCTTTCTGATGATGATGAACTTTCATCAC -3' (*EhSNX1*); 5'-GAAAGATCTATGAGTAATTATGCACAGTATGAATA -3' and 5'-GAAAGATCTCCAACTAGTAACTTCCCAATTGTCTT -3' (*EhSNX2*), where restriction enzyme sites are underlined. Amplified fragments were digested by *Bgl*II (NEBiolabs) and ligated into pEhEx-HA vector. To construct plasmids for gene silencing of *EhSNX1* and *EhSNX2* gene, the initial 420 bp of the *EhSNX1* coding region and full-length (426 bp) of *EhSNX2* were PCR amplified with the following primers: 5'- GAAAGGCCTATGGGAGATAATAAAGAAGATATTAT -3' and 5'- GAAGAGCTCTTGACTTCTTAATGACTGAAATTGAG -3' (*EhSNX1*); 5'-GAAAGGCCTATGAGTAATTATGCACAGTATGAATA -3' and 5'-GAAGAGCTCTTACCAACTAGTAACTTCCCAATTGT -3' (*EhSNX2*). These PCR fragments were digested by *Stu*I (NEBiolabs) and *Sac*I, and ligated into *Stu*I- and *Sac*I-double digested psAP2-Gunma vector (Mi-ichi *et al*., 2011; Penuliar *et al*., 2011). These plasmids were designated as psAP2-SNX1 and psAP2-SNX2. To construct plasmids to express EhArpC3 with FLAG tag fused at the amino terminus, the full-length protein coding sequence of these genes was amplified by PCR with the following primers: 5'-GAACCCGGGATGACCACAATTGCCAAACAAGATAA -3' and 5'-GAACTCGAGTTAAATGGTTTTGTTTAAGAACTTTC -3' (*EhArpC3*), where restriction enzyme sites are underlined. Amplified fragments were digested by *Xma*I and *Xho*I, and ligated into pEhEx-FLAG vector, to produce pEhEx-FLAG-ArpC3.

2-1-5 Establishment of *E. histolytica* transformants

The trophozoites of HM-1:IMSS cl6 were transfected with pEhExHA-SNX1, pEhExHA-SNX2, pEhExGFP-SNX1, pEhExGFP-SNX2, pEhEx-FLAG-ArpC3, pEhExHA, pEhExGFP, and pEhExFLAG, respectively, while the trophozoites of G3 strain were transfected with psAP2-SNX1, psAP2-SNX2, and psAP2, respectively, by lipofection as previously described (Nozaki *et al*., 1999). Geneticin was added at a concentration of 1 μg/mL, 24 hr after transfection then gradually until the transfection control cells (transfected without plasmid) were killed and the geneticin concentration reached 10μg/mL. The production of the *E. histolytica* line that expresses GFP-HrsFYVE with c-myc tag at the amino terminus under tetracycline induction was previously described (Nakada-Tsukui *et al*., 2009).

2-1-6 Immunoblot analysis

Approximately 10^5 trophozoites were harvested in the exponential growth phase, washed twice with phosphate buffer saline (PBS), pH 7.4 and resuspended in 50 μl of lysis buffer (50 mM Tris-HCl, pH 7.5, 150 mM NaCl, 1% Triton X-100), 50 μg/mL of E-64, and complete mini), Approximately 20μg of the total cell lysate were separated on 12% SDS-polyacrylamide gels and subsequently electrotransferred onto nitrocellulose membranes. The membranes were incubated with 5% non-fat dried milk in Tris-Buffered Saline and Tween-20 (TBS-T) (50 mM Tris-HCl, pH8.0, 150 mM NaCl and 0.05% Tween-20) for 30 min. The proteins were respectively reacted with primary mouse antibodies specific for HA (with the dilution of 1:1000), myc (1:1000), GFP (1:100), FLAG (1:1000), and rabbit antisera against EhVps26 (1:100), EhVps35 (1:500), EhCP-A5 (1:1000), and CS1 (1:1000) at 4ºC overnight. After the reaction with the primary antibodies, the membranes were washed with TBS-T three times, ant they were further reacted with HRP-conjugated anti-mouse or anti-rabbit IgG antiserum (1:6000 or 1:8000, respectively) at room

temperature for 1 hr. After washing with TBS-T three times, the specific proteins were visualized with chemiluminescence detection using Immobilon Western Chemiluminescent HRP Substrate (Millipore corporation, Massachusetts, USA) according to the manufacturer's protocol.

2-1-7 Phagosome purification

Paramagnetic Dynabeads of 2.8 μm diameter (Invitrogen, California, USA) were incubated with human serum (Sigma Aldrich) for 16 hr at 4ºC, washed, and re-suspended in transfection medium [OPTI-MEM I medium (Thermo Fisher), adjusted to pH 6.8, containing 5 mg/ml L-cysteine and 1 mg/ml ascorbic acid]. Approximately 2.4×10^7 trophozoites were transferred to each well on 6-well plates (Corning, New York, USA) and incubated at 35.5ºC for 30 min to allow the trophozoites to attach to the surface of the well. After the medium was removed, 2 ml transfection medium containing approximately 1×10^7 human serum-coated beads were added to each well (at the ratio 10 beads per amoeba cell). Beads were immediately sedimented on the surface of the amoebae that were seeded on the well by centrifugation at 100 *g* at room temperature for 5 min. Transfection medium was removed and 3 ml of warm BIS was added. The plates were further incubated at 35.5ºC for 30 min. After incubation, the medium was removed and 3 ml of cold PBS was added to each well of the plates. The plates were put on ice for 10 min to detach amoebae and the amoebae were washed twice with cold PBS. After centrifugation at 800 *g* at 4ºC for 3 min, the supernatant was removed and the amoebae were resuspended in 500 μl of 8 mg/mL dithiobis(succinimidyl propionate) (DSP) solution (Thermo Fisher, Massachusetts, USA), containing 0.5 mM of β-glycerophosphate, 0.1 mM of EDTA, 10 mM sodium fluoride, and 1 mM sodium orthovanadate. The mixture was incubated on a rotator (10 rpm) at 4ºC for 30 min. To quench the reaction, 50 μl of 1 M Tris-HCl, pH 7.5 was added and the mixture was further incubated as above for 10 min. After the amoebae were treated with DSP, they were washed with

homogenization buffer [250 mM sucrose, 3 mM imidazole, in PBS, pH 7.4, and complete mini (Sigma Aldrich)]. Cells were mechanically disrupted by applying 25-70 strokes of a Dounce homogenizer. The homogenate was centrifuged at 800 *g* at 4ºC for 3 min to remove unbroken cells. Bead-containing phagosomes were concentrated from the lysates by magnetic separation on PureProteome Magnetic Stand (Merck). The phagosomes were washed five times with 500 µl of homogenization buffer containing protease inhibitors and lysed with 10 µl of lysis buffer (50 mM Tris-HCl, pH 7.5, 150 mM NaCl, 1% Triton X-100) containing 50 µg/ml of E-64, and cOmplete mini). For immunoblot analysis, approximately 20 µg of phagosomes were resuspended in SDS-PAGE sample buffer (0.25 M Tris-HCl, pH 6.8, 8% SDS, 8% 2-mercaptoethanol, 40% glycerol, 0.004% bromophenol blue), boiled for 5 min, and subjected to SDS-PAGE.

2-1-8 Lipid overlay assay

Approximately 6×10^6 *E. histolytica* cells were harvested and washed with PBS. Approximately 150 µl of lysis buffer (50 mM Tris-HCl, pH 7.5, 150 mM NaCl, 1% Triton X-100, 0.05 mg/mL E-64, and Complete Mini) was added to an approximately 100 µl bed volume of the pellet. The mixtures were incubated on ice for 30 min and centrifuged at 16,000 *g* for 5 min. The total cell lysate (supernatant) was collected after centrifugation. Nitrocellulose membranes on which various phosphoinositides and other lipids had been spotted (PIP strips: P-6001, Echelon Biosciences, Salt Lake City, USA) were treated with 1 % fatty acid-free bovine serum albumin (BSA) (Sigma Aldrich) in PBS-T (PBS containing 0.05 % Tween 20) for 1 hr at room temperature for blocking. The membranes were incubated with 2 ml of the lipid binding solution (PBS-T containing 1% fatty acid free BSA and Complete Mini) containing 20-fold diluted amebic lysates for 2 hr at 4ºC. After incubation with amoebic lysates, the membranes were washed with PBS-T three times at 4ºC. The membranes were then reacted with anti-HA mouse monoclonal (with the

dilution of 1:500), anti-myc mouse monoclonal (1:500), anti-GFP mouse monoclonal (1:100) antibodies, anti-EhVps26 (1:100), and anti-EhVps35 rabbit antisera (1:500), at 4ºC for 3 hr. After the membranes were washed twice with PBS-T at 4ºC, they were further reacted with HRP-conjugated anti-mouse or anti-rabbit IgG antiserum (1:6000 or 1:8000, respectively) at 4ºC for 1 hr. After washing three times with PBS-T at 4ºC, the specific proteins were visualized by chemiluminescence detection using Immobilon Western Chemiluminescent HRP Substrate (Millipore corporation, Massachusetts, USA) according to the manufacturer's protocol.

2-1-9 Quantitative real-time PCR

The levels of *EhSNX1* and *EhSNX2* gene transcripts were analyzed by quantitative real-time PCR. PolyA RNA was extracted, cDNA was prepared, and PCR was performed with cDNA as a template, as previously described (Mitra *et al*., 2007). RNA polymerase II served as an internal control (GenBank accession number, XP_649091) (Gilchrist *et al*., 2006). PCR was performed using the following primer sets: sense primer, 5'-CCTGGTTATAGATTTAAACCAGAATTTACTGAACA -3' and antisense primer, 5'-GAACTCGAGTTATTCTGATGATGATGAACTTTCAT -3' for *EhSNX1*; sense primer 5'-TCGGTACAATCCCACCTCTTCCCTGGAGATACAATC -3' and antisense primer 5'-GAACTCGAGTTACCAACTAGTAACTTCCCAATTGT -3' for *EhSNX2* and the following cycling parameters: an initial step of denaturation at 95ºC for 20 sec, followed by 40 cycles of denaturation at 95ºC for 3 sec, then annealing and extension at 60ºC for 30 sec.

2-1-10 Staining of CHO cells

After CHO cells were cultured as described above on 10-cm diameter plastic dishes (IWAKI) for 2 days (before reaching confluence), they were incubated with CellTracker Blue CMAC

Dye (Thermo Fisher) at the final concentration of 10 μM at 37 ºC for 30 min. CHO cells were detached from the surface of the flasks by treating with PBS containing 0.5 mg/ml trypsin and 0.2 mM EDTA at 37ºC for 5 min, washed twice with PBS, and re-suspended in 600 μl of transfection medium per 3×10^6 CHO cells harvested from one dish.

2-1-11 Immunoflorescence assay (IFA)

Approximately 5×10^3 *E. histolytica* trophozoites were incubated with 5×10^4 Dynabeads M-280 Tosylactivated beads (Invitrogen, California, USA) or 5×10^4 CHO cells, which had been pre-stained with CellTracker Blue as described below, in 50 μl BI-S-33 medium in 8-mm round wells on a slide glass at 35.5ºC for 15 min. Cells were fixed with 3.7% paraformaldehyde and subsequently permeabilized with 0.2% saponin in PBS containing 1% bovine serum albumin for 10 min each at room temperature. The cells were reacted with anti-HA mouse antibody (with the dilution of 1:1000) or anti-Vps26 rabbit antibody (1:1000) as previously described (Nakada-Tsukui *et al*., 2005). After washing with PBS three times, the cells were reacted with Alexa Fluor-488 anti-mouse secondary antibody (1:1000) and Alexa Fluor-568 anti-rabbit secondary antibody (1:1000) (Thermo Fisher), respectively. The samples were observed using Carl-Zeiss LSM 780 Meta laser-scanning confocal microscope. The resultant images were further analyzed using Zen software (Carl-Zeiss, Oberkochen, Germany).

2-1-12 Live imaging and quantification of GFP-fused EhSNXs

Approximately 7×10^4 trophozoites of the amoeba transformants transfected with pEhExGFP-SNX1, pEhExGFP-SNX2, or pEhExGFP were respectively cultured on a 3.5-cm diameter glass bottom dish in BIS medium under reduced oxygen using Anaerocult (Merck). After the medium was removed, approximately 7×10^5 CHO cells were added to the dish at the ratio of 10 CHO cells per amoeba, and the center part of the glass bottom was covered by a cover slip. Live

imaging was performed using a Carl Zeiss LSM780 (Land Baden-Wurttemberg, Germany) with default settings on the time series mode. Images captured were analyzed by ZEN software (Carl Zeiss). The recruitment of GFP-EhSNX1/2 to phagosomes and trogosomes was estimated by quantitating the fluorescence intensity of a region of interest (ROI) on the phagosome membrane and the neighboring cytoplasm. The average intensity per pixel of the ROI was calculated. The ratio of the fluorescence intensity of GFP-EhSNX1/2 on the phagosome membrane against that in the cytosol was calculated and referred as the relative fluorescent signal on the membrane.

2-1-13 Cross linking and immunoprecipitation of HA-tagged EhSNXs and native EhVps26

Approximately 1×10^6 trophozoites of the amoeba transformants transfected with pEhExHA-SNX1, pEhExHA-SNX2, pEhExSNX1-HA, pEhExSNX2-HA, or pEhExHA were cultured on a 10-cm diameter dish in BIS medium with reduced oxygen using Anaerocult (Merck). CHO cells were added to the dish at the ratio of 10 CHO cells per amoeba and the dish was incubated at 35.5ºC for 30 min. After the medium containing uningested CHO cells was removed, the amoebae were detached from the surface of the dish by adding cold PBS into the dish and incubating them on ice for 10 min. After the trophozoites were washed with PBS three times, the cell pellet was cross linked with DSP as described above. After washing twice with PBS, the cells were lysed with 800 µl of lysis buffer (50 mM Tris-HCl, pH7.5, 15 mM NaCl, containing 1% Triton X-100, 0.05 mg/mL E-64, and complete mini). After the debris was removed by centrifugation at 16,000 *g* at 4ºC for 5 min, the lysates were mixed and incubated with 50 µl of Protein G Sepharose beads (GE Healthcare, Illinoi, USA) (80 % slurry) at 4ºC for 1 hr. After centrifugation at 800 *g* at room temperature for 3 min, the supernatant was transferred to a new 1.5-ml microtube containing either approximately 50 µl (80% slurry) of anti-HA monoclonal antibody produced in mouse, clone HA-7, purified immunoglobulin conjugated to agarose beads (Sigma Aldrich) or 50 µl of protein G

Sepharose (GE Healthcare), which was treated with 250 µl of PBS, 2 µl of anti-Vps26 rabbit antiserum for 1hr at 4ºC. The mixtures were incubated with inversion at 4ºC for 3.5 hr and then centrifuged at 800 *g* to separate unbound proteins. The beads were washed three times with 1 ml of lysis buffer. After washing, the beads were resuspended in 180 µl of lysis buffer containing HA-peptide at the final concentration of 0.2 mg/ml and the mixture was incubated at 4ºC overnight to elute the bound proteins for HA-EhSNXs or directly boiled with 50 µl of 2x SDS-PAGE sample buffer for EhVps26.

2-1-14 Quantification of trogocytosis and phagocytosis using image cytometer

Approximately 3×10^5 trophozoites were incubated in 6 mL of BIS medium containing 10 µM CellTracker Green for 30 min at 35.5ºC. CHO cells were stained with 10 µM CellTracker Blue as described above. Approximately 1×10^5 trophozoites were seeded onto a 3.5-cm diameter glass bottom dish in 2 mL of BIS medium and incubated for 20 min. For trogocytosis measurement, after removing the supernatant, approximately 1×10^5 CHO cells in 90 µl BIS medium were added onto the 1.0-cm diameter glass central pit of the dish. For phagocytosis measurement, CHO cells were killed by incubating at 55ºC for 15 min, and added to the pit of the dish. After the pit was covered with a cover glass, the mixture was cultivated at 35.5ºC under anaerobic conditions. The images were taken on a Confocal Quantitative Image Cytometer, CQ1 (Yokogawa Electric Corporation, Tokyo, Japan) every 10 min for 80 min. The volume of the ingested CHO cells (blue) was calculated using three dimensionally reconstituted data. To analyze these data using 3 dimensional structured images, CQ1 was set as below. At first, the top and bottom positions of Z-stack containing almost all phagosomes were set. The number of slices depends on distance between layers should be less than 4 µm. The images were further analyzed to quantify the volume and the fluorescence intensity of the ingested CHO cells using the CellPathfinder high content analysis

software (Yokogawa Electric Corporation).

2-2 Results

2-2-1 Identification of class I PI3-kinases

Among PI3-kinases, the members of Class I PI3-kinases predominantly produce $PI(3,4,5)P_3$ from $PI(4,5)P_2$. There are two kinds of class I PI3-kinases based on the composition of their catalytic and regulatory subunits. One of the three class IA catalytic subunits (p110α, β, and δ) associates with one of the five p85 class regulatory subunits (p85α, p85β, p55α, p55γ, and p50α), while the class IB catalytic subunit (p110γ) associates with one of the two P101/p87 class regulatory subunits (p101 and p87) (Vadas *et al*., 2011; Jean & Kiger, 2014) (Fig. 2, left side). In mammals, p110α and p110β are expressed ubiquitously, while p110δ and p110γ seem to be restricted to hematopoietic cells. The class IA catalytic subunits (p110α, β, and δ) are activated via receptor tyrosine kinases and generate $PI(3,4,5)P_3$ at the plasma membrane, while the p110β and p110γ catalytic subunits are activated downstream of the G protein-coupled receptor (GPCR) (Stephens *et al*., 1994; Stoyanov *et al*., 1995; Vanhaesebroeck *et al*., 2010a).

Independent of the query used, ten proteins were identified to share significant overall similarity, reflecting a possible redundancy among them (E-value < 1×10^{-10}) in *E. histolytica* (Table 1). Six of them have conserved domains, such as Ras binding domain (RBD), C2, lipid kinase unique (LKU), and PI3-kinase catalytic domains, but no protein with the adaptor binding domain (ABD) was identified (Fig. 2, right side). I tentatively designated the proteins that contain LKU and catalytic domains as class I PI3-kinases, since they cannot be further classified into p110α, β, γ, or δ. Also, no homologues of the regulatory subunits that contain Src homology 2 (SH2) domain were identified in the *E. histolytica* genome database when p85α, β, p55α, p50α, and p55γ were used as queries.

2-2-2 Absence of detectable class II PI3-kinase homologues *in E. histolytica*

Class II PI3-kinases are monomeric enzymes that generate PI(3,4)P_2 and PI3P from PI4P and PI, respectively (Balla, 2013; Maffucci and Falasca, 2014). There are three subtypes: PI3-kinase C2α, β, and γ, among which PI3-kinase C2α and β have N-terminal extensions that are likely involved in autoinhibition and protein-protein interactions with clathrin (Marat and Haucke, 2016). Except for the N-terminal extensions, all class II PI3-kinases contain one RBD, two C2, one LKU, one catalytic, and one PX domains. PI3-kinase C2α and β isoforms are ubiquitously expressed, whereas the γ isoform is largely restricted to the liver.

In *E. histolytica*, I could not detect any class II PI3-kinase homologues. When three human class II PI3-kinases were used as queries, the best hits I obtained were the same proteins identified as class I PI3-kinases. As described above, because of the low similarity to class II PI3-kinases in five out of six candidates and the absence of the PX domain in all the six, they were classified into class I PI3-kinases. Additionally, class II PI3-kinases evolved after Metazoa, and another amoeboid organism, *D. discoideum*, lacks this class of PI3-kinases (Engelman *et al*., 2006; Brown and Auger, 2011). Together, these suggest that there are no class II PI3-kinases in *E. histolytica*. However, the conservation of a gene showing low E-value with the class II PI3-kinase, hints at a possibility that some of the class I PI3-kinases have a role similar to that of class II PI3-kinases.

2-2-3 Identification of class III PI3-kinase

The human genome has one class III PI3-kinase, Vps 34, which phosphorylates the D3-position of PI. Vps34 consists of one of each of the C2, helical, and catalytic domains, and forms a dimer with the p150 regulatory subunit (Vps15 in yeast). p150 constitutively interacts with Vps34, and the myristoyl modification in its amino terminal links Vps34 to the membrane (Stack *et al*., 1993; Vanhaesebroeck *et al*., 2010a). Vps34 participate in membrane trafficking, endocytosis,

phagocytosis, and autophagy through the synthesis of PI3P (Sasaki *et al*., 2009; Swanson, 2014; Wallroth and Haucke, 2018; also see section 1.2.2).

In *E. histolytica*, homologues of Vps34 (EHI_096560) and p150 (EHI_044190) were detected. The structure of EhVps34 is similar to class I PI3-kinases in *E. histolytica* which conserved C2, LKU, and catalytic domain (Fig. 2). EHI_096560 was the top hit obtained from the BLAST search using human Vps34 as a query (E-value = 2×10^{-87}) (Table 1). The second hit in the Vps34 BLAST result was EHI_006130 which was the top hit of class I PI3-kinase BLAST search (query:NP_006209, E-value = 1.6×10^{-131}). I identified EHI_096560 as a Vps34 homologue from these results.

2-2-4 *E. histolytica* possesses a highly divergent PTEN homologue

PTEN is predominantly localized to the cytosol, and also dynamically associated with the plasma membrane, where it hydrolyzes PI(3,4,5)P_3 (Billcliff and Lowe, 2014). Although PTEN lacks a nuclear localization signal, it is localized to the nucleus and plays important roles in chromosome stability by directly interacting with centromere specific binding protein C (CENP-C), DNA repair by interacting with p53 and Rad51, and cell cycle regulation by interacting with APC and MAP kinases.(Trotman *et al*., 2007; Chung and Eng, 2005; Chung *et al*., 2006; Tang and Eng, 2006a; Tang and Eng, 2006b; Shen *et al*., 2007; Song *et al*., 2011; Freeman *et al*., 2003).

PTEN consists of a PI3- or PI 4-phosphatase domain (Ptase), a C2 domain, two PEST (proline, glutamine, serine, threonine) sequences, and a PDZ domain (Fig. 3). The C2 domain is known to be involved in lipid binding and protein stability. PEST sequences are known to enhance proteolytic sensitivity, and the PDZ domain is involved in protein-protein interactions (Maehama, 2007; Sasaki *et al*., 2009; Balla, 2013). The human genome encodes three isotypes of TPIP, and only two of them have an N-terminal transmembrane domain (Fig. 3). The *E. histolytica* genome potentially encodes six PTEN orthologues with E-values less than 1×10^{-10} to the human PTEN (Table 2).

2-2-5 MTMs are conserved in *E. histolytica* but are not classified into some groups

MTMs preferentially dephosphorylate PI3P and PI(3,5)P_2. The human MTM family consists of 15 members [MTM1 and MTM related (MTMR) 1–14]. MTMs are categorized into six groups based on their domain configurations and catalytic activity: MTM1 and MTMR1–2; MTMR3–4; MTMR6–8; MTMR14; MTMR5 and 13; and MTMR9–12 (Fig. 3). The phosphatase domain contains a CX_5R motif that is overall well-conserved in MTMs. Among the 15 MTMs, six of them (MTMR5 and MTMR9-13) substituted the conserved cysteine and arginine residues within the CX_5R motif with other amino acids, and thus these MTMs are catalytically inactive (Hus and Mao, 2015; Laporte *et al*., 2003; Hnia *et al*., 2012). In all MTMs, except for MTMR14, the PH-GRAM (pleckstrin homology-glucosyltransferase, Rab-like GTPase activator and myotubularin) domain is conserved. This domain is involved in PI binding. Additionally, they all have an active or inactive catalytic core, and a coiled-coil domain, which is involved in homo- or hetero-dimerization. In addition, some members have a C-terminal PDZ binding sequence and a FYVE domain. The N-terminal DENN and C-terminal PH domains are conserved in two of the catalytically inactive MTM members, MTMR5 and MTMR13. Although all the catalytically inactive members (MTMR5 and MTMR9–13) lack an active phosphatase domain, they can heterodimerize with active MTMs, whereby inactive MTMs likely regulate the activity and localization of active MTMs (Lorenzo *et al*., 2006; Kim *et al*., 2003; Mochizuki *et al*., 2003). The role of MTMs in endocytosis and membrane traffic has been well-characterized (Hohendahl *et al*., 2016; Robinson and Dixon, 2006).

Genome-wide survey against the *E. histolytica* genome using human MTM1, MTMR3, 5, 6, 9, or 14 as queries respectively, identified an identical set of 11 proteins with E-values $<1\times10^{-58}$ (Table 2). I concluded that 10 out of these 11 potential homologues are *E. histolytica* MTM

orthologues by Pfam search, because they contain a myotubularin-like phosphatase domain. All of them, except EHI_188050 and EHI_140980, contain the conserved catalytic domain (Fig. 3). The phosphatase domains of these two exceptions contains a conserved cysteine residue in their C(S/T)DGWDR motifs, but arginine is replaced with serine (CRNGWDS) or isoleucine (CIDGTGI), respectively. Although *E. histolytica* MTMs appear to have a simpler domain organization, they also are thought to heterodimerize as in model organisms given that the genome contains both active and inactive MTMs.

2-2-6 Identification of retromer complex components as potential PI3P effectors that were recruited to phagosomes

The enzymes related to the phosphorylation at the inositol ring exist in *E. histolytica.* The results of the *in silico* search indicated that all PIPs exist in *E. histolytica*, suggesting PIPs are needed for survival of this organisms. Among all PIPs, we focused on PI3P because PI3P may have an important role in phago/trogocytosis in amoeba. PI3P is localized on phago/trogosomes, but the PI3P effector required in downstream mechanisms remains unknown. To identify PI3P-binding effectors that are involved in phagosome biogenesis in *E. histolytica*, particularly during the late stage of maturation, we opted to utilize differential proteomic analysis of the phagosomes under normal *vs.* PI3P-deprived (competed) conditions. We rationalized that overexpression of a soluble PI3P-binding protein should compete with other PI3P effectors that play roles in phagosome maturation to be recruited (Fig. 4a). To this end, the *E. histolytica* strain that expresses GFP fused-HrsFYVE, which is a well-documented human PI3P binding domain (Nakada-Tsukui et al., 2009), in a tetracycline-inducible fashion, was established. Expression of GFP-HrsFYVE in *E. histolytica* peaked at 24 hr of cultivation with 10 μg/ml of tetracycline (Fig. 4b). At this time point, I confirmed by immunofluorescence assay that GFP-HrsFYVE was localized on the phagosomes containing

human serum-coated Dynabeads (Fig. 4c). I verified the purity of the phagosome-enriched fraction by the significant enrichment of GFP-HrsFYVE (Fig. 4d) and the mature CP-A5 in the phagosome enriched fraction. Altogether, these results suggest that my protocol of phagosome purification using serum-coated Dynabeads allowed us to successfully enrich phagosomes that were associated with GFP-HrsFYVE and thus PI3P, on phagosome membranes (Fig. 4c). I isolated phagosomes using previously established protocols (Marion et al., 2005) and analyzed their proteome under the conditions of GFP-HrsFYVE being expressed and non-expressed. After all detected proteins were categorized by their functions, those detected at least two-fold higher under the GFP-HrsFYVE non-expressed condition compared with those under the GFP-HrsFYVE expressed condition were considered to be potential candidates of PI3P binding proteins. Only proteins categorized to lipid metabolism and vesicular trafficking are shown in Figure 4e. Among them, vacuolar protein sorting (Vps) 26 and Vps35, both of which are the components of the retromer complex, were detected, which were mainly investigated in this study.

2-2-7 *In silico* identification of SNX in *E. histolytica*

In mammalian cells, the retromer complex is known to be involved in recycling of transmembrane receptors from endosomes to the trans-Golgi network (Bonifacino & Hurley, 2008). It has been demonstrated that the retromer complex consists of two subcomplexes: the major subcomplex of Vps26/Vps29/Vps35 and a combination of SNX1 or 2, SNX5 or 6, and SNX3. The retromer is recruited to PI3P-rich endosomes via PX domain of SNX3 (Seaman, 2012). The components of the major subcomplex (Vps26/Vps29/Vps35) have been identified and investigated in *E. histolytica* (Nakada-tsukui, et al., 2005; Picazarri et al., 2015; Srivastava et al., 2017). However, it remains elusive whether or not SNXs are also conserved in *E. histolytica* and if they are, what is the role of SNXs in vesicular traffic, particularly during phagocytosis and trogocytosis.

There are several classes of SNXs known in mammals: those with PX and BAR (Bin/Amphiphysin/Rvs) domains, those with PX domain and other domain such as FERM, PDZ, and SH3 domains, and those containing PX domain only (Worby & Dixon, 2002). Human SNX1 or SNX3 belongs to the first or third group, respectively (Cullen, 2008). Human SNX3 is responsible for recruiting the retromer complex to the membrane of late endosomes via binding to PI3P (Seaman, 2012). Human SNX3 is phosphorylated on Ser72 (Lenoir *et al*., 2018). When phosphorylated, it cannot bind to PI3P and is localized to the cytosol.

I conducted an *in silico* survey of *SNX* genes in the *E. histolytica* genome. I used sorting nexin 1 isoform a (NP_003090.2) from *Homo sapiens* as a query for Blastp and identified two proteins encoded by EHI_060320 and EHI_004400 as possible SNX homologues (E-value of 4×10^{-6} and 1×10^{-4}, respectively). Both of the proteins have PX domain but lack any other recognizable domains, thus, based on domain configuration, are considered to be orthologous to human SNX3. These *E. histolytica* SNX orthologues were designated as EhSNX1 and EhSNX2. Alignment of EhSNX1, EhSNX2, and human SNX3 protein sequences shows that the residue corresponding to the conserved Ser72 (conserved among about the half of human SNXs) is present in the PX domain of EhSNX1 (Ser132) and EhSNX2 (Ser53) (Fig. 5). Two out of four residues shown to be involved in the binding to PI3P are conserved in EhSNX1 and EhSNX2. Three out of ten residues implicated in the binding to Human Vps26 and Vps35 are conserved in EhSNX1, but not in EhSNX2, suggesting a possibility of isotype-specific interactions with EhVps26 and EhVps35. It is also worth noting that EhSNX1, but not EhSNX2, has an approximately 60 amino acid-long amino terminal extension and a 10 amino acid-long carboxyl terminal extension rich in serine and negatively charged amino acids, which may be involved in protein-protein interaction.

2-2-8 PIP binding specificity of EhSNX1/2

To investigate whether EhSNX1 and EhSNX2 bind to PIPs and, if so, what PIP species they bind, I established *E. histolytica* lines that expressed EhSNX1 and EhSNX2 with HA tag at the N-terminal. A single band corresponding to the expected molecular mass of HA-EhSNX1 (27.7 plus 3 kDa for the HA tag) or HA-EhSNX2 (17.0 plus 3 kDa for the HA tag) was observed in the respective transformants (Fig. 6a). The lipid overlay assay using amebic lysates from these transformants showed that both EhSNX1 and EhSNX2 specifically bound to PI3P (Fig. 6b). I also verified the lipid binding activity of some PI3P binding protein candidates in the proteome list (Fig. 4e) such as β-adaptin, Vps35, Vps26, and Syntaxin, by lipid overlay assay. However, they did not bind to any phospholipids including PI and PIPs (data not shown).

2-2-9 Localization of HA tagged EhSNX1/2 in steady state and during trogocytosis

As EhSNXs were shown to bind to PI3P and thus, work as PI3P effectors, their localization is expected to be in PI3P-rich membranes (compartments) during phago- and trogocytosis. Since it was not clear whether EhSNXs form a complex with the other major retromer subcomplex, I investigated whether EhSNXs are co-localized with Vps26 during trogocytosis of CHO cells by immunofluorescence assay (IFA) using HA-EhSNX1 and HA-EhSNX2 expressing strains. In steady state, both EhSNX1 and EhSNX2 were localized on some small vesicles associated with EhVps26 (Fig. 7, a and b). To investigate the localization and kinetics of EhSNXs during trogocytosis, I performed IFA at 15 min after addition of CellTracker Blue-stained live CHO cells to *E. histolytica* trophozoites. EhSNX1 was localized on the bottom of the trogocytic cup associated with EhVps26 (Fig. 7a). EhSNX1 appeared to be dissociated from the trogosome after trogocytic cup membrane was closed (data not shown, see below for live imaging quantitation). Unlike EhSNX1, EhSNX2 was seldom present on the pre-closure trogocytic cup, but localized on

the closed trogosomes associated with EhVps26 (Fig. 7b).

2-2-9 Time-lapse analysis of the trogosome localization of GFP-EhSNX1/2

I monitored and quantified (Fig. 8) GFP-EhSNX1/2 on the trogocytic cup (and tunnel-like structures) and the trogosome during trogocytosis, according to the protocol described in Material and Methods. GFP-EhSNX1 was recruited to the trogocytic cup when the cup was formed, and remained associated until 108 sec (note that the movie started to be recorded 4-7 sec after adherence) (Fig. 8). The intensity of GFP-EhSNX1 was detected after the attachment of the trophozoite to the CHO cell and gradually decreased during trogosome maturation. On the contrary, GFP-EhSNX2 was recruited to the trogosome after the trogocytic cup was enclosed. The signal of GFP-EhSNX2 remained low until 108 sec; it suddenly increased at 124 sec (Fig. 8). This live imaging suggests sequential processes in which GFP-EhSNX2 recruitment to the trogosome occurred after GFP-EhSNX1 dissociation from the trogosome.

2-2-10 Immunoprecipitation of EhSNX1/2 using anti-EhVps26 antibody

To demonstrate physical interaction between EhSNX1/2 and the EhVps26-containing the retromer complex during trogocytosis, immunoprecipitation was performed with anti-EhVps26 antiserum using lysates from EhSNX1-HA expressing cells. Expression of EhSNX1-HA was confirmed by immunoblot using anti-HA antibody (Fig. 9a). For unknown reasons, EhSNX2-HA-expressing transformant could not be established (data not shown), and HA-EhSNX2 was used as control. Since EhSNX1 was found on the trogocytic cup/trogosome during trogocytosis of CHO cells, EhSNX1-HA-expressing cells were co-incubated with CHO cells for 30 min and subjected to immunoprecipitation with anti-EhVps26 antiserum and immunoblot analysis using anti-HA antibody, anti-EhVps26, and anti-EhVps35 antisera. EhVps26, EhVps35, and, in a lesser amount,

EhSNX1-HA were immunoprecipitated from EhSNX1-HA-expressing cells (Fig. 9b). HA-EhSNX2 was not co-precipitated with EhVps26, suggesting that the interaction with EhVps26 was specific to EhSNX1, but not EhSNX2.

2-2-11 Immunoprecipitation demonstrates interaction between EhSNX1 and actin related protein (Arp) 2/3 complex component

To further understand the role of EhSNX1, immunoprecipitation was performed using the strain expressing EhSNX1 with the amino-terminal HA. HA-EhSNX1 was immunoprecipitated with anti HA-agarose after co-incubation with CHO cells for 30 min. One specific band around 20 kDa was detected after SDS-PAGE and silver staining (Fig. 10a), and subjected to MS analysis (Fig. 10b). Notably, two of eight detected proteins (EHI_174910; EHI_030820) were C3 and C4 components of actin-related protein (Arp) 2/3 complex. To verify the interaction, the strain expressing FLAG-tagged 2/3 complex subunit 3 (EhArpC3) (FLAG-EhArpC3) was established. The FLAG-EhArpC3 localization was examined by IFA using anti-FLAG antibody. FLAG-EhArpC3 was localized on the tunnel-like structure (corresponding to the neck of a flask) during trogocytosis of CHO cells (Fig. 10c). On the other hand, EhVps26 was never found on the tunnel-like structure, but on the bottom region of the trogocytic cup (before closure) and on the trogosome (after closure).

2-2-12 Establishment of *EhSNX1/2* gene silencing strains

To better understand how EhSNXs are involved in trogo- and phagocytosis, I performed transcriptional gene silencing (gs) of *EhSNX1* and *EhSNX2* genes. In the parental G3 line transformed with the mock vector, the level of *EhSNX2* mRNA is approximately 3.0 fold higher than that of *EhSNX1*. The level of *EhSNX1* transcript was reduced by 81 % due to *EhSNX1* gene

silencing, while that of *EhSNX2* was conversely increased by 41 % (Fig. 11a). In contrast, the level of *EhSNX1* and *EhSNX2* transcripts was reduced by 55 % and 94 % by *EhSNX2* gene silencing, respectively (Fig. 11a).

2-2-13 Quantification of trogosome recruitment of Vps26 and trogocytosis/phagocytosis efficiency of *EhSNX1/2* gene silencing strains

Since EhSNX1 physically interacts with the major retromer subcomplex (see above), gene silencing of *EhSNX*s can potentially affect localization of the complex during trogo- and phagocytosis and also efficiency of ingestion. EhVps26 was swiftly recruited, together with EhSNX1, to the trogocytic cup during trogocytosis of CHO cell (Fig. 7a). Almost all (96%) of CHO cell-containing trogosomes in the control strain were decorated with EhVps26 at 10 min of co-incubation with CHO cells (Fig. 11b). At 30 min, a slightly less proportion (81%) of trogosomes in the control were still decorated with EhVps26. Although statistically insignificant (p-value 0.44 and 0.11, at 10 and 30 min, respectively), gene silencing of *EhSNX1* caused less recruitment of EhVps26 to trogosomes compared with the control (4% and 14% reduction compared to the control at 10 and 30 min, respectively). Gene silencing of *EhSNX2* caused no change in the association of EhVps26 with trogosomes at 10 and 30 min. Next, I measured the total volume of ingested CHO cells per trophozoite, in *EhSNX1*gs, *EhSNX2*gs, and mock strains, on image cytometer CQ1, to estimate the efficiency of trogocytosis. The data shown are the average of the volumes of all trogosomes per amoeba in 3 wells each. The amoebic transformants were cultivated with CHO cells and images were captured every 10 min for 80 min. Interestingly, trogocytosis significantly increased by 1.4-2.0 fold in *EhSNX2*gs strain compared to the control at all time points (p value<0.05) (Fig. 11c). On the other hand, the volume of ingested CHO cells was not changed in *EhSNX1*gs strain at any time point. Phagocytosis was also affected by *EhSNX2* gene silencing; the

volume of ingested pre-killed CHO cells increased by 1.4-2.0 fold in *EhSNX2*gs strain at all time points, similar to the effects on trogocytosis (Fig. 12).

2-3 Discussion

2-3-1 *E. histolytica* conserved six of class I PI3-kinases but not class II PI3-kinases

Based on *in silico* analysis, *E. histolytica* possesses six class I PI3-kinases, but the regulatory subunit is not conserved. In *Saccharomyces cerevisiae,* class I and II PI3-kinases are not conserved. *Dictyostelium discoideum* has the catalytic but not the regulatory subunits of three class I PI3-kinases and lacks class II PI3-kinases (Engelman *et al*, 2006). The catalytic subunits of *D. discoideum* class I PI3-kinases also lack the ABD as in *E. histolytica.* Such lineage-specific modifications of the catalytic subunits and loss of the regulatory subunits of class I PI 3-kinases likely suggest divergence of $PI(3,4,5)P_3$-mediated lipid signaling in eukaryotes.

Furthermore, only five proteins were predicted to have an SH2 domain. four of them were annotated as protein kinases, while the remaining protein was predicted to have a role in RNA stability and/or transcriptional regulation, with no possible link to PI3-kinase regulatory subunits. These data suggest the possibility that the regulatory subunits of class I PI3-kinase have been lost or replaced with a lineage-specific protein in *E. histolytica* during evolution.

2-3-2 Class III PI3-kinase provides PI3P from PI in *E. histolytica*

Class III PI3-kinase called Vps34 is conserved in *E. histolytica*. The domain structure of EhVps34 (EHI_096560) is the same as mammalian Vps34. Vps34 is first characterized as a protein related to vesicular transport in yeast. The regulatory subunit, Vps15, also exists in *E. histolytica* with almost the same length and domain structure (presence of the kinase domain as a

serine/threonine kinase like general Vps15) as the human homologue. These results suggest that class III PI3-kinase in *E. histolytica* may work as a PI3-kinase and that PI3P is provided from PI using this kinase. Since Vps34 is the only PI3-kinase in yeast, and is also widely conserved in the Eukaryota, Vps34 is considered to be the ancestral PI3-kinase (Stack *et al.*,1993; Engelman *et al.*, 2006; Brown & Auger, 2011).

2-3-3 PI3-phosphatases are the most diversified PIP-related enzymes in *E. histolytica*

E. histolytica has six PI(3,4,5)P_3 phosphatase homologues of PTEN, while there is only one PTEN gene in the human genome (Fig. 3, Table2). It suggests that PI3-phosphatases are very diversified in *E. histolytica.* Domain search by Pfam showed that six PTEN orthologues contain the CX_5R motif-containing phosphatase domain. Furthermore, the same protein candidates were detected when the three human TPIP isoforms were used as queries. The E-values against TPIP were around 1×10^{-16}–10^{-17}, which is higher than those against PTEN. Thus, I concluded that they are likely PTEN orthologues. Three of the *E. histolytica* PTEN orthologues also had a C2 domain. In the other three *E. histolytica* PTEN candidates that lack the C2 domain, only a few residues are conserved (four in EHI_010360, EHI_054460; three in EHI_041900). Thus, it is not clear if the three C2 domain-lacking *E. histolytica* PTEN candidates have functional cytosol localization signals.

Members of the Amoebozoa supergroup exclusively have a protein family that contain multiple inactive myotubularin domains. These proteins have been designated as inactive myotubularin/LRR/ROCO/kinase (IMLRK) proteins (Kerk & Moorhead, 2010). Nine IMLRK proteins have previously been identified in the *E. histolytica* genome by the FFAS03 (Fold and Function Assignment System) sequence: profile method and the HHPred [Hidden Markov Model (HMM)-HMM structure prediction] profile: profile method (Kerk & Moorhead, 2010). The *D.*

discoideum homologues of IMLRKs, Pats1 and GbpC, have been identified as a cytokinesis-related protein and cGMP-binding protein, respectively (Pomorski *et al*., 2003; Goldberg *et al*., 2002). Since both *D. discoideum* IMLRK homologues are involved in cytoskeleton-related processes such as cytokinesis and chemotaxis, *E. histolytica* IMLRKs may also be involved in the similar processes (Pomorski *et al*., 2003; Bosgraaf *et al*., 2002; Bosgraaf *et al*., 2005; Lewis, 2009). However, it is not clear why *E. histolytica* has inactive myotubularin domains, and more IMLRK proteins than *D. discoideum* (nine vs. two, respectively).

2-3-4 EhSNX1/2 are downstream effectors of PI3P signals on the trogosome membrane

PIPs-mediated signaling plays a pivotal role in phago- and trogocytosis in *E. histolytica.* In this study, we identified for the first time the retromer complex, in particular SNXs, as a PI3P downstream effector on the phago- and trogosome membrane in *E. histolytica.* It has been well established that in mammalian cells, PI3P is recruited to phago- and trogosomes after complete closure of the phago/trogocytic cup and formation of the phago/trogosome, and that PI3P effectors such as EEA1 is recruited to the enclosed phagosomes to facilitate maturation of phago/trogosomes. It has been shown in *E. histolytica* that PI3P is localized on the phagocytic cup before closure as well as on the enclosed phagosomes (Nakada-Tsukui *et al*., 2009) and the timing of PI3P recruitment to the phago- and trogocytic cup in *E. histolytica* appears to be different from human cells (Yeung & Sergio, 2007). However, as no known PI3P effector homologues were found in the *E. histolytica* genome, role of PI3P on the phago/trogocytic cup and phago/trogosomes and its downstream effectors remained elusive. To identify the proteins which are recruited to phagosomes in a PI3P-dependent manner, we took a unique approach using our unique reverse genetic system in which PI3P-binding Hrs-FYVE domain fused with GFP, expressed in a tetracycline-inducible manner, competes with endogenous PI3P binding proteins for PI3P on phago- and trogosomes.

Since such interaction between PI3P and its effectors is transient and unstable, we needed to use a cross-linker and a phosphatase inhibitor to immobilize such interaction (Fig. 13).

SNXs were not identified from *E. histolytica* in our previous study by biochemical approaches (Nakada-tsukui *et al*., 2005). Furthermore, *in silico* gene survey also failed to identify SNX homologues (Nakada-tsukui *et al*., 2005), which was likely due to the use of yeast Vps5p as a query for BLAST search. *E. histolytica* SNXs were identified when human either SNX1 or SNX3 was used as a query, but not by using PX domain from another protein as a query (the E-values of the BLASTp search using HsSNX1 or HsSNX3 as a query were: 4e-6 and 5e-10 for EHI_060320, respectively; 1e-04 and 3e-13 for EHI_004400; whereas that using yeast Vps5p was 0.007 for EHI_060320 and 0.002 for EHI_004400).

2-3-5 PIP specificity of EhSNX1/2 and human SNXs

The PIP binding specificity of EhSNX1 and EhSNX2 compared to that of human SNX1, 2, and 3 is intriguing. In humans, there are more than 30 members of SNXs known (Cullen, 2008) and only several members have known PIP binding specificity. Human SNX1 and SNX2 showed preference in the order of PI(3,4,5)P_3>PI(3,5)P_2>PI3P and PI3P>PI4P>PI5P, respectively, while human SNX3 almost exclusively binds to PI3P, similar to EhSNX1 and EhSNX2 (Worby & Dixon, 2002). Amino acid alignment shows six amino acid residues that are shared by EhSNX1, EhSNX2, and HsSNX3, but not conserved in both HsSNX1 and HsSNX2, including EhSNX1 T107 of (EhSNX2 T28), EhSNX1 Y131 (EhSNX2 Y53), EhSNX1 L160 (EhSNX2 L82), EhSNX1 G162 (EhSNX2 G84), EhSNX1 F175 (EhSNX2 F96), and EhSNX1 I191 (EhSNX2 I112) (Fig. 14). The conservation of EhSNX1 G162 (EhSNX2 G84) corresponding to HsSNX3 G94 is of particular interest as these residues are also exclusively present in HsSNX11-13 and 27 (Lenoir *et al*., 2018), among which PIP specificity of only HsSNX13 was shown: preferred binding to PI3P and PI5P

over PI(3,5)P_2 and PI4P (Worby & Dixon, 2002). These data suggest that EhSNX1 G162 (EhSNX2 G84) potentially contributes to PI3P specificity. While PIP specificity may be affected by domains other than the PX domain, for those proteins that contain multiple domains such as HsSNX13 (Cullen, 2008), those of EhSNX1 and EhSNX2 are likely to be attributable only to the PX domain, similar to HsSNX3.

2-3-6 EhSNX1 and EhSNX2 have different roles during trogocytosis

The two SNXs from *E. histolytica* have similar domain structure (containing only PX domain, but lacking BAR domain) and lipid binding specificities, but showed distinct patterns of localization and trogo-/phagosome recruitment, and phenotypes by gene silencing. We have shown by biochemical, genetic analyses and live imaging that EhSNX1, but not EhSNX2, is involved in the recruitment of EhVps26 during trogocytosis. We have also shown that EhSNX2 is negatively involved in trogocytosis per se, as demonstrated with partial augmentation of trogocytosis by *EhSNX2* gene silencing. Our data indicate, together with our previous finding showing that EhVps26 of the retromer complex is recruited to the trogocytic cup (Nakada-tsukui *et al*., 2005; Picazarri *et al*., 2015), that EhSNX1 recruits the retromer complex to the trogo/phagosome in a PI3P-dependent manner. Unlike EhSNX1, EhSNX2 did not interact with the retromer complex as indicated. This result is consistent with the fact that the amino acid residues implicated for the binding with the retromer complex are not conserved in EhSNX2 (see Fig. 5).

The fact that gene silencing of *EhSNX2*, but not *EhSNX1,* increased the trogocytosis efficiency was counter-intuitive, and suggestive of EhSNX2 being a negative regulator of trogocytosis. It has been shown that in dendritic cells, SNX3 overexpression causes defect in early endosome maturation by competition in PI3P binding on early endosomes and reduction of EEA1 recruitment (Chua & Wong, 2013). This observed phenotype may mirror the apparent upregulation

of trogocytosis by *EhSNX2* gene silencing. However, the loss of competition for PI3P by *EhSNX2* gene silencing may not be the reason of the observed upregulation of trogocytosis because no change in trogocytosis was observed by *EhSNX1* gene silencing, which in theory also causes reduced competition for PI3P. The lack of phenotype by *EhSNX1* gene silencing may be explained at least in part by compensatory upregulation of *EhSNX2* gene expression by *EhSNX1* gene silencing. One possible scenario to explain these phenotypic changes in both human and *E. histolytica* is that both HsSNX3 and EhSNX2 employ a possible negative downstream effector/machinery needed for maturation of early endosomes and trogosomes.

2-3-7 EhSNX1 binds to Arp2/3 complex for downstream signaling to cytoskeletal rearrangement during trogocytosis

We demonstrated that EhSNX1 specifically bound to ArpC3/ArpC4 of the Arp2/3 complex. ArpC3 and ArpC4 were found to interact with EhSNX1 as indicated by LC/MS/MS analysis of the immunoprecipitated samples using HA-EhSNX1 as a bait. In general, Arp2/3 complex is known to be composed of seven subunits and involved in elongation, branching, and crosslinking of actin filaments via regulation of actin nucleation and elongation (Goley & Welch, 2006). Since all components of the Arp2/3 complex were found in the previous phagosomal proteome analyses (Okada *et al*., 2006; Marion *et al*., 2005; Furukawa *et al*., 2013; Boettner *et al*., 2008), the Arp2/3 complex was suggested to be involved in phago- and trogocytosis. The recruitment of EhSNX1 to the trogocytosis initiation site was specific to EhSNX1 and not observed for EhSNX2. Precise timing of the recruitment of EhSNX1 to the trogocytosis initiation site relative to that of Arp2/3 was not determined as live imaging was unable to be performed. However, the recruitment of EhSNX1 appeared to slightly precede that of Arp2/3. The continuity of the association of EhSNX1 and Arp2/3 clearly indicates close and direct interplay between them,

triggered by PI3P-dependent recruitment of EhSNX1 to the trogocytosis initiation site. It is worth noting that the localization of EhVps26 and EhArpC3 on the trogocytic cup were overlapping but not identical. Together with the observation that EhSNX1 partially colocalized with EhVps26, these observations indicate that EhSNX1 may play a role in bridging the cytoskeletal rearrangement by EhArpC3 and receptor recycling mediated by the retromer.

2-3-8 Proposed model of amoebic trogocytosis based on EhSNX1/2 live imaging

Based on the biochemical, live imaging, and immunofluorescence image data, we propose the following model of how key players are engaged with trogocytosis (Fig. 15). Upon the adherence of the amoebic trophozoite to the live mammalian cell, PI3P is locally synthesized in situ on the trogocytosis initiation site. EhSNX1 is recruited via PI3P binding mediated by its PX domain to the trogocytosis initiation site, which then becomes the trogocytic cup. EhSNX1 recruits Arp2/3 complex, which subsequently leads to actin cytoskeleton reorganization needed for the establishment of the tunnel-like structure of the trogosomes and also the closure of the trogosomes. At the same time, EhSNX1 also recruits the retromer complex via interaction with Vps26. The retromer complex then binds to the hydrolase receptors for the retrieval (and recycling) of the receptors. Once the trogocytic cup (or the trogosome) is enclosed, EhSNX2 is recruited to the trogosome by virtue of its PI3P binding ability with a concomitant dissociation of EhSNX1. This model depicts a sequential involvement of EhSNX1 and EhSNX2 during the formation and maturation of trogosomes.

The apparent enhancement of trogocytosis by *EhSNX2* gene silencing is possibly due to a loss of negative feedback regulation toward the initial trogocytosis event(s) as explained above. However, its mechanism and the possible negative effector(s) remain elusive and need further investigation. The recruitment of EhSNX1 and 2 to the trogocytic cup and the trogosome was time-

and localization (domain)-specific. Although the underlying mechanism of the spaciotemporal recruitment of EhSNXs remains unknown, it is plausible that phosphorylation of the conserved Ser72 (of HsSNX3) (Figure S3) may regulate the binding of EhSNX1/2 to PI3P and other possible accessory and effector proteins in an isotype-specific manner.

The retromer complex was previously identified as an effector of GTP-bound active Rab7A in *E. histolytica* (Nakada-tsukui *et al*., 2005). EhRab7A was reported to be localized to the preparatory vacuolar organelle that emerges upon erythrophagocytosis (pre-phagosomal vacuole, PPV), where EhRab7A and EhVps26 were co-localized. In this study, the effects of *EhSNX1* gene silencing on the inhibition of Vps26 recruitment to the trogosome was not large and rather marginal, suggesting that the recruitment of the retromer may be also regulated via EhRab7A.

Acknowledgement

I would like to express my deepest gratitude to my supervisor, Dr. Kumiko Nakada-Tsukui (National Institute of Infectious Disease) for insightful advises and comments throughout my study. I also thank Dr. Tomoyoshi Nozaki (The university of Tokyo), Dr. Kisaburo Nagamune (National Institute of Infectious Disease, University of Tsukuba), Dr. Tetsuo Hashimoto (University of Tsukuba), Dr. Yuji Inagaki (University of Tsukuba), and Dr. Herbert Santos (The university of Tokyo) for critical comment and support. I thank all the members of the laboratory for valuable discussions and help. I would like to thank Dr. Tomohiko Maehama for supporting doing lipid experiments and analysis.

Reference

Balla, T. (2013). Phosphoinositides: Tiny lipids with giant impact on cell regulation. *Physiological Reviews*, *93*(3), 1019–1137. https://doi.org/10.1152/physrev.00028.2012

Boettner, D. R., Huston, C. D., Linford, A. S., Buss, S. N., Houpt, E., Sherman, N. E., & Petri, W. a. (2008). Entamoeba histolytica phagocytosis of human erythrocytes involves PATMK, a member of the transmembrane kinase family. *PLoS Pathogens*, *4*(1), e8. https://doi.org/10.1371/journal.ppat.0040008

Bonifacino, J. S., & Hurley, J. H. (2008). Retromer. *Current Opinion in Cell Biology*, *20*(4), 427–436. https://doi.org/10.1016/j.ceb.2008.03.009

Bosgraaf, L., Russcher, H., Smith, J. L., Wessels, D., Soll, D. R., & Van Haastert, P. J. M. (2002). A novel cGMP signalling pathway mediating myosin phosphorylation and chemotaxis in Dictyostelium. *EMBO Journal*, *21*(17), 4560–4570. https://doi.org/10.1093/emboj/cdf438

Bosgraaf, L., Waijer, A., Engel, R., Visser, A. J. W. G., Wessels, D., Soll, D., & van Haastert, P. J. M. (2005). RasGEF-containing proteins GbpC and GbpD have differential effects on cell polarity and chemotaxis in Dictyostelium. *Journal of Cell Science*, *118*(9), 1899–1910. https://doi.org/10.1242/jcs.02317

Bracha, R., Nuchamowitz, Y., & Mirelman, D. (2003). Transcriptional silencing of an amoebapore gene in Entamoeba histolytica: Molecular analysis and effect on pathogenicity. *Eukaryotic Cell*, *2*(2), 295–305. https://doi.org/10.1128/EC.2.2.295-305.2003

Brown, J. R., & Auger, K. R. (2011). Phylogenomics of phosphoinositide lipid kinases: Perspectives on the evolution of second messenger signaling and drug discovery. *BMC Evolutionary Biology*, *11*(1), 1–14. https://doi.org/10.1186/1471-2148-11-4

Chua, R. Y. R., & Wong, S. H. (2013). SNX3 recruits to phagosomes and negatively regulates phagocytosis in dendritic cells. *Immunology*, *139*(1), 30–47.

https://doi.org/10.1111/imm.12051

Cullen, P. (2008). Endosomal sorting and signalling: an emerging role for sorting nexins : Abstract : Nature Reviews Molecular Cell Biology. *Nature Reviews Molecular Cell Biology*, *9*(7), 574–582. Retrieved from http://www.nature.com/nrm/journal/v9/n7/abs/nrm2427.html;jsessionid=2B6040A2FF75C8EA809BE493E30C2D52

Diamond, L. S., Mattern, C. F. T., & Bartgis, I. L. (1972a). Viruses of Entamoeba histolytica. I. Identification of transmissible virus-like agents. *Journal of Virology*, *9*(2), 326–341.

Engelman, J. A., Luo, J., & Cantley, L. C. (2006). The evolution of phosphatidylinositol 3-kinases as regulators of growth and metabolism. *Nature Reviews Genetics*, *7*(8), 606–619. https://doi.org/10.1038/nrg1879

Furukawa, A., Nakada-tsukui, K., & Nozaki, T. (2013). Cysteine Protease-Binding Protein Family 6 Mediates the Trafficking histolytica. *Infection and Immunity*, *81*(5), 1820–1829. https://doi.org/10.1128/IAI.00915-12

Gilchrist, C. A., Houpt, E., Trapaidze, N., Fei, Z., Crasta, O., Asgharpour, A., … Petri, W. A. (2006). Impact of intestinal colonization and invasion on the Entamoeba histolytica transcriptome. *Molecular and Biochemical Parasitology*, *147*(2), 163–176. https://doi.org/10.1016/j.molbiopara.2006.02.007

Goldberg, J. M., Bosgraaf, L., Van Haastert, P. J. M., & Smith, J. L. (2002). Identification of four candidate cGMP targets in Dictyostelium. *Proceedings of the National Academy of Sciences of the United States of America*, *99*(10), 6749–6754. https://doi.org/10.1073/pnas.102167299

Goley, E. D., & Welch, M. D. (2006). The ARP2/3 complex: an actin nucleator comes of age. *Nature Reviews Molecular Cell Biology*, *7*(10), 713–726. https://doi.org/10.1038/nrm2026

Jean, S., & Kiger, A. A. (2014). Classes of phosphoinositide 3-kinases at a glance. *Journal of Cell*

Science, *127*(5), 923–928. https://doi.org/10.1242/jcs.093773

Kerk, D., & Moorhead, G. B. G. (2010). A phylogenetic survey of myotubularin genes of eukaryotes: Distribution, protein structure, evolution, and gene expression. *BMC Evolutionary Biology*, *10*(1). https://doi.org/10.1186/1471-2148-10-196

Lenoir, M., Ustunel, C., Rajesh, S., Kaur, J., Moreau, D., Gruenberg, J., & Overduin, M. (2018). Phosphorylation of conserved phosphoinositide binding pocket regulates sorting nexin membrane targeting. *Nature Communications*, *9*(1), 1–12. https://doi.org/10.1038/s41467-018-03370-1

Lewis, P. A. (2009). The function of ROCO proteins in health and disease. *Biology of the Cell*, *101*(3), 183–191. https://doi.org/10.1042/bc20080053

Lucas, M., Gershlick, D. C., Vidaurrazaga, A., Rojas, A. L., Bonifacino, J. S., & Hierro, A. (2016). Structural Mechanism for Cargo Recognition by the Retromer Complex. *Cell*, *167*(6), 1623-1635.e14. https://doi.org/10.1016/j.cell.2016.10.056

Malek, M., Kielkowska, A., Chessa, T., Anderson, K. E., Barneda, D., Pir, P., … Stephens, L. R. (2017). PTEN Regulates PI(3,4)P2 Signaling Downstream of Class I PI3K. *Molecular Cell*, *68*(3), 566-580.e10. https://doi.org/10.1016/j.molcel.2017.09.024

Marat, A. L., & Haucke, V. (2016). Phosphatidylinositol 3-phosphates—at the interface between cell signalling and membrane traffic. *The EMBO Journal*, *35*(6), 561–579. https://doi.org/10.15252/embj.201593564

Marion, S., Laurent, C., & Guillén, N. (2005). *Signalization and cytoskeleton activity through myosin IB during the early steps of phagocytosis in Entamoeba histolytica : a proteomic approach*. *Cellular Microbiology*,*7*(10), 1504–1518. https://doi.org/10.1111/j.1462-5822.2005.00573.x

Mi-ichi, F., Makiuchi, T., Furukawa, A., Sato, D., & Nozaki, T. (2011). Sulfate activation in

mitosomes plays an important role in the proliferation of entamoeba histolytica. *PLoS Neglected Tropical Diseases*, *5*(8), 1–7. https://doi.org/10.1371/journal.pntd.0001263

Mitra, B. N., Saito-Nakano, Y., Nakada-Tsukui, K., Sato, D., & Nozaki, T. (2007). Rab11B small GTPase regulates secretion of cysteine proteases in the enteric protozoan parasite Entamoeba histolytica. *Cellular Microbiology*, *9*(9), 2112–2125. https://doi.org/10.1111/j.1462-5822.2007.00941.x

Nakada-Tsukui, K., Okada, H., Mitra, B. N., & Nozaki, T. (2009). Phosphatidylinositol-phosphates mediate cytoskeletal reorganization during phagocytosis via a unique modular protein consisting of RhoGEF/DH and FYVE domains in the parasitic protozoon Entamoeba histolytica. *Cellular Microbiology*, *11*(10), 1471–1491. https://doi.org/10.1111/j.1462-5822.2009.01341.x

Nakada-tsukui, K., Saito-nakano, Y., Ali, V., & Nozaki, T. (2005). *A Retromerlike Complex Is a Novel Rab7 Effector That Is Involved in the Transport of the Virulence Factor Cysteine Protease in the Enteric Protozoan Parasite Entamoeba histolytica*. *16*(11), 5294–5303. https://doi.org/10.1091/mbc.E05

Nozaki, T., Asai, T., Sanchez, L. B., Kobayashi, S., Nakazawa, M., & Takeuchi, T. (1999). Characterization of the Gene Encoding Serine Acetyltransferase, a Regulated Enzyme of Cysteine Biosynthesis from the Protist ParasitesEntamoeba histolytica and Entamoeba dispar. Regulation and possible function of the cysteine biosynthetic pathway in Entamoeba. *Journal of Biological Chemistry*, *274*(45), 32445–32452. https://doi.org/10.1074/jbc.274.45.32445

Nozaki, Tomoyoshi, Asai, T., Sanchez, L. B., Kobayashi, S., Nakazawa, M., & Takeuchi, T. (1999). Characterization of the Gene Encoding Serine Acetyltransferase, a Regulated Enzyme of Cysteine Biosynthesis from the Protist Parasites Entamoeba histolytica and Entamoeba dispar. *Journal of Biological Chemistry*, *274*(45), 32445–32452.

https://doi.org/10.1074/jbc.274.45.32445

Okada, M., Huston, C. D., Oue, M., Mann, B. J., Petri, W. A., Kita, K., & Nozaki, T. (2006). Kinetics and strain variation of phagosome proteins of Entamoeba histolytica by proteomic analysis. *Molecular and Biochemical Parasitology*, *145*(2), 171–183. https://doi.org/10.1016/j.molbiopara.2005.10.001

Penuliar, G. M., Furukawa, A., Sato, D., & Nozaki, T. (2011). Mechanism of trifluoromethionine resistance in Entamoeba histolytica. *Journal of Antimicrobial Chemotherapy*, *66*(9), 2045–2052. https://doi.org/10.1093/jac/dkr238

Picazarri, K., Nakada-Tsukui, K., Tsuboi, K., Miyamoto, E., Watanabe, N., Kawakami, E., & Nozaki, T. (2015). Atg8 is involved in endosomal and phagosomal acidification in the parasitic protist Entamoeba histolytica. *Cellular Microbiology*, *17*(10), 1510–1522. https://doi.org/10.1111/cmi.12453

Pomorski, T., Lombardi, R., Riezman, H., Devaux, P. F., Meer, G. Van, & Holthuis, J. C. M. (2003). Drs2p-related P-type ATPases Dnf1p and Dnf2p Are Required for Phospholipid Translocation across the Yeast Plasma Membrane and Serve a Role in Endocytosis. *Molecular Biology of the Cell*, *14*(3), 1240–1254. https://doi.org/10.1091/mbc.e02-08-0501

Ralston, K. S., Solga, M. D., MacKey-Lawrence, N. M., Somlata, Bhattacharya, A., & Petri, W. A. (2014). Trogocytosis by Entamoeba histolytica contributes to cell killing and tissue invasion. *Nature*, *508*(7497), 526–530. https://doi.org/10.1038/nature13242

Sasaki, T., Takasuga, S., Sasaki, J., Kofuji, S., Eguchi, S., Yamazaki, M., & Suzuki, A. (2009). Mammalian phosphoinositide kinases and phosphatases. *Progress in Lipid Research*, *48*(6), 307–343. https://doi.org/10.1016/j.plipres.2009.06.001

Seaman, M. N. J. (2012). The retromer complex - endosomal protein recycling and beyond. *Journal of Cell Science*, *125*(20), 4693–4702. https://doi.org/10.1242/jcs.103440

Somlata, Nakada-Tsukui, K., & Nozaki, T. (2017). AGC family kinase 1 participates in trogocytosis but not in phagocytosis in Entamoeba histolytica. *Nature Communications*, *8*(1), 1–12. https://doi.org/10.1038/s41467-017-00199-y

Srivastava, V. K., Yadav, R., Watanabe, N., Tomar, P., Mukherjee, M., Gourinath, S., … Datta, S. (2017). Structural and thermodynamic characterization of metal binding in Vps29 from Entamoeba histolytica: implication in retromer function. *Molecular Microbiology*, *106*(4), 562–581. https://doi.org/10.1111/mmi.13836

Stack, J. H., Herman, P. K., Schu, P. V., & Emr, S. D. (1993). A membrane-associated complex containing the Vps15 protein kinase and the Vps34 PI 3-kinase is essential for protein sorting to the yeast lysosome-like vacuole. *EMBO Journal*, *12*(5), 2195–2204.

Swarbrick, J. D., Shaw, D. J., Chhabra, S., Ghai, R., Valkov, E., Norwood, S. J., … Collins, B. M. (2011). VPS29 is not an active metallo-phosphatase but is a rigid scaffold required for retromer interaction with accessory proteins. *PLoS ONE*, *6*(5). https://doi.org/10.1371/journal.pone.0020420

Vadas, O., Burke, J. E., Zhang, X., Berndt, A., & Williams, R. L. (2011). Structural biology structural basis for activation and inhibition of class I phosphoinositide 3-kinases. *Science Signaling*, *4*(195), 1–13. https://doi.org/10.1126/scisignal.2002165

Vanhaesebroeck, B., Guillermet-Guibert, J., Graupera, M., & Bilanges, B. (2010). The emerging mechanisms of isoform-specific PI3K signalling. *Nature Reviews. Molecular Cell Biology*, *11*(5), 329–341. https://doi.org/10.1038/nrm2882

Walker, S. M., Downes, C. P., & Leslie, N. R. (2001). TPIP: A novel phosphoinositide 3-phosphatase. *Biochemical Journal*, *360*(2), 277–283. https://doi.org/10.1042/0264-6021:3600277

Worby, C. A., & Dixon, J. E. (2002). SORTING OUT THE CELLULAR FUNCTIONS OF

SORTING NEXINS. *Nature Reviews. Molecular Cell Biology*, *3*, 919–931.

Yeung, T., & Sergio, G. (2007). *Lipid signaling and the modulation of surface charge during phagocytosis*. *219*, 17–36. https://doi.org/10.1111/j.1600-065X.2007.00546.x

Yousuf, M. A., Mi-Ichi, F., Nakada-Tsukui, K., & Nozaki, T. (2010). Localization and targeting of an unusual pyridine nucleotide transhydrogenase in Entamoeba histolytica. *Eukaryotic Cell*, *9*(6), 926–933. https://doi.org/10.1128/EC.00011-10

Figures and tables

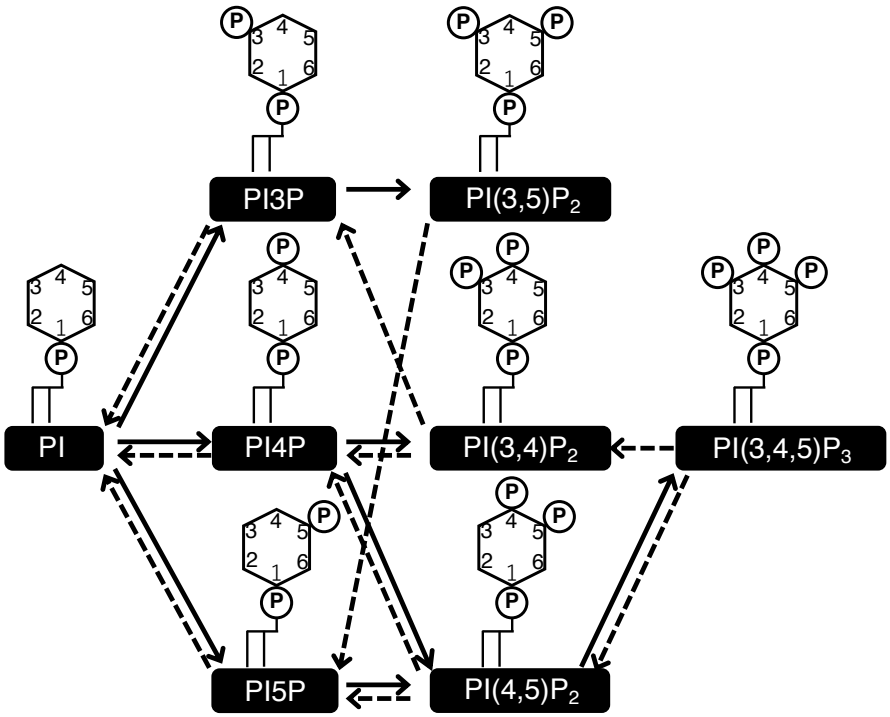

Figure 1. Structures of phosphatidylinositol and phosphoinositides, and the routes of their interconversion

PtdIns consists of a glycerol backbone with two covalently attached fatty acids at the *sn-1* and *sn-2* positions, and a D-*myo*-inositol head group linked via the phosphate at the *sn-3* position. Three hydroxyl groups of the D-*myo*-inositol head group (D3-5) are independently phosphorylated or dephosphorylated to form the seven kinds of phosphorylated PtdIns, PIs. Solid and broken arrows indicate kinase and phosphate reactions, respectively.

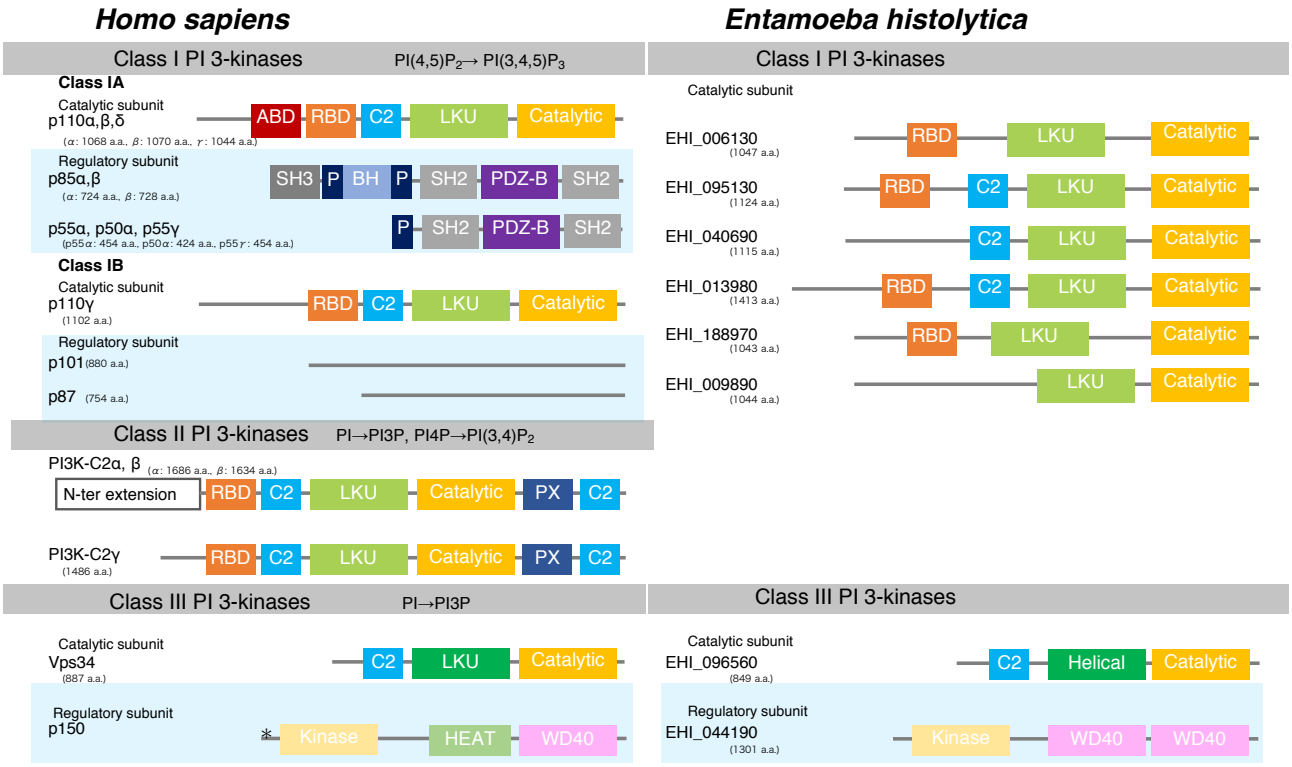

Figure 2. Structural features of PI kinases of *H. sapiens* and *E. histolytica*. Structural features and domain organization of PI kinases, including their regulatory subunits are shown. Numbers showing at the end of the protein or after the name of the protein indicates amino acid length. Abbreviations: adaptor binding domain (ABD); Ras binding domain (RBD); C2 domain (C2); lipid kinase unique domain (LKU); lipid kinase domain of PI 3- and PI 4-kinases (Catalytic); kinase core domain of PIP kinases (PIPKc); Ser kinase domain (Kinase); Src homology 2 (SH2); Src homology 3 (SH3); Proline-rich (P); Bcl Homology (BH); PDZ domain binding domain (PDZ-B); Phox homology (PX); Huntington, Elongation factor3, PR65/A, and TOR (HEAT); WD40 repeat (WD40). Myristoylation site is depicted with "*".

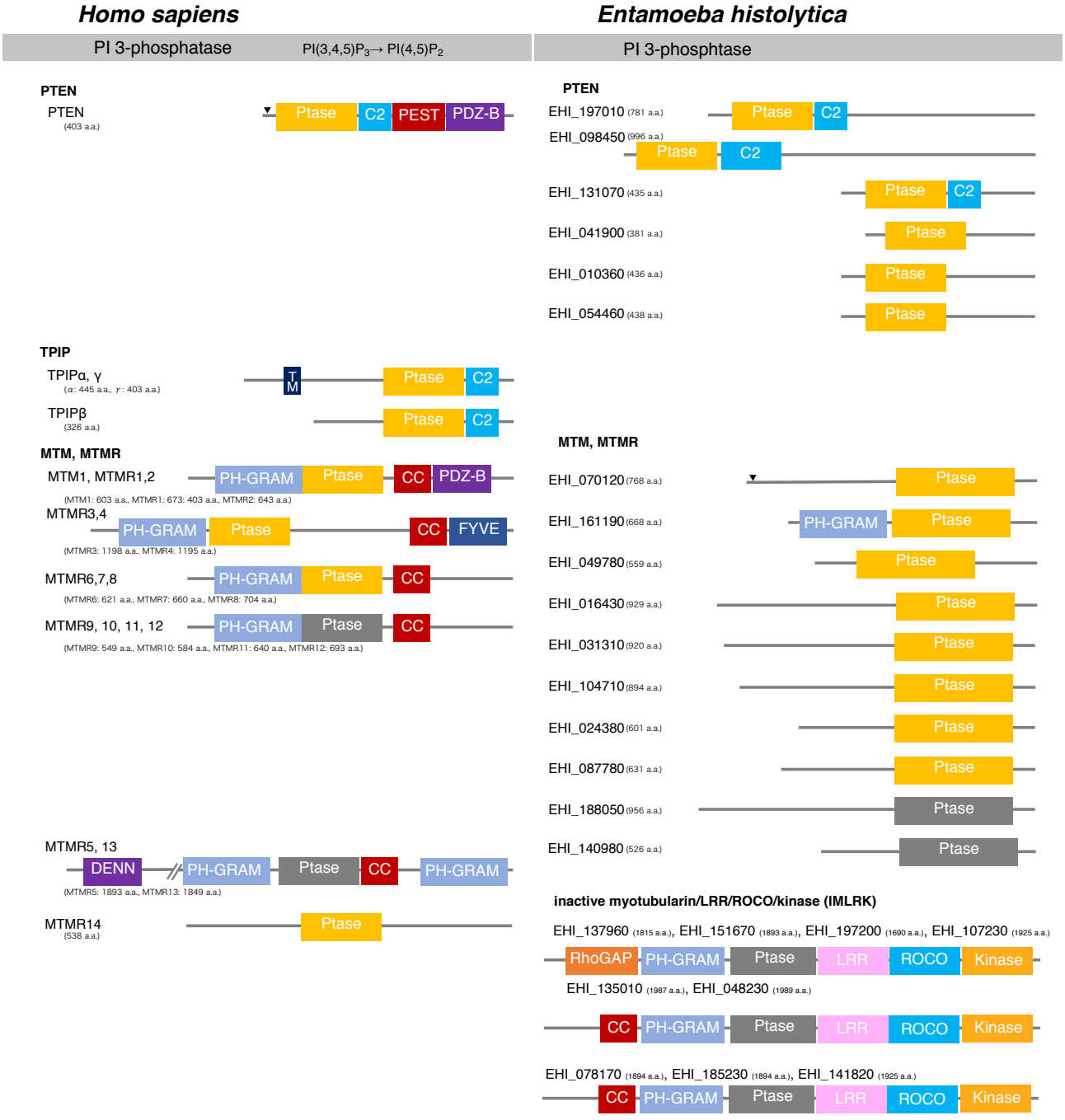

Figure 3. Structural features of PI phosphatases of *H. sapiens* and *E. histolytica*. Structural features and domain organization of the PI phosphatases are shown. Abbreviations: active CX_5R motif containing PI 3- or PI 4-phosphatase domain (Ptase; yellow); inactive Ptase domain (Ptase; gray); Proline, glutamine, serine, threonine (PEST); coiled coil domain (CC); differentially expressed in normal versus neoplastic (DENN); glucosyltransferases Rab-like GTPase activators and myotubularins (GRAM); transmembrane domain (TM); leucine-rich repeats (LRR); comprised of a ROC (Ras of complex proteins) and COR (C-terminal of ROC) region (ROCO). The nuclear localization signal is labeled with "▼".

(a)

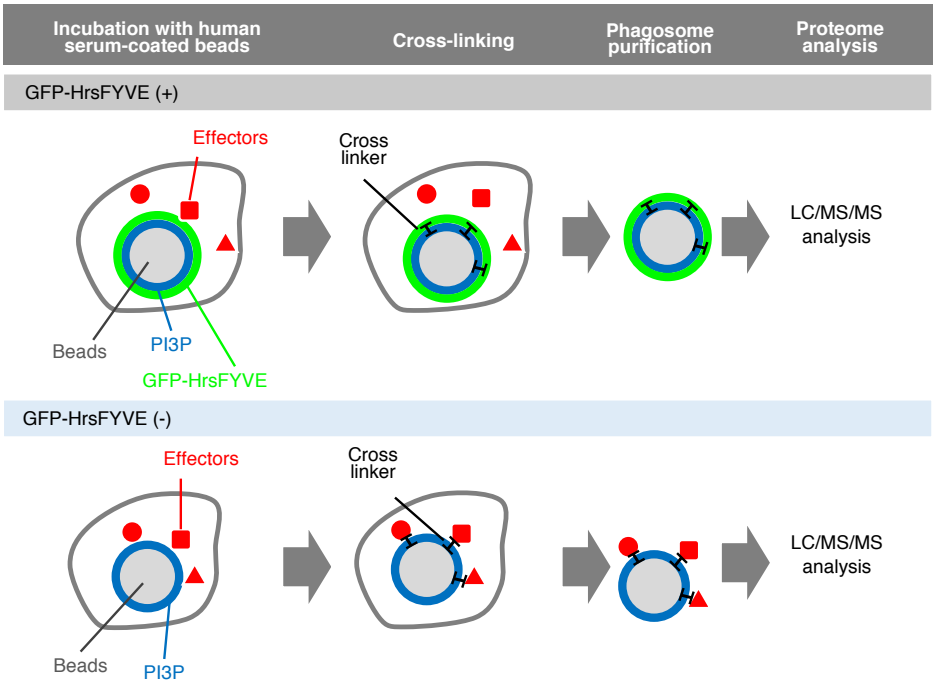
Incubation with human serum-coated beads
Cross-linking
Phagosome purification
Proteome analysis
GFP-HrsFYVE (+)
Effectors
Cross linker
LC/MS/MS analysis
Beads
PI3P
GFP-HrsFYVE
GFP-HrsFYVE (-)
Effectors
Cross linker
LC/MS/MS analysis
Beads
PI3P

(b)

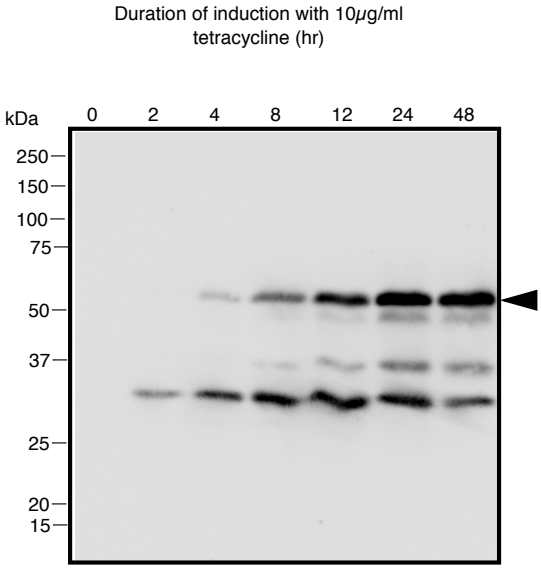
Duration of induction with 10μg/ml tetracycline (hr)
kDa
0
2
4
8
12
24
48
250
150
100
75
50
37
25
20
15

(c)

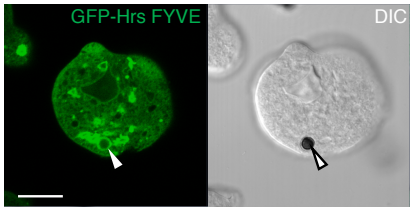

(d)

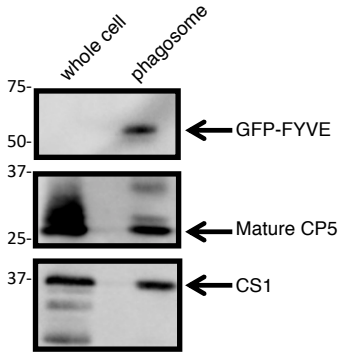

(e)

name of proteins	accession number	MW	tet(+)	tet(-)	tet(-)/tet(+)
Lipid binding and metabolism					
Putative uncharacterized protein	EHI_040420	56 kDa	1.23	3.36	2.73
Phosphatidylinositol 3-kinase, putative	EHI_095130	130 kDa	1.23	3.36	2.73
Putative uncharacterized protein	EHI_197010	91 kDa	1.23	3.36	2.73
Putative uncharacterized protein	EHI_080260	26 kDa	2.47	5.89	2.39
PH domain containing protein	EHI_117920	47 kDa	2.47	5.05	2.05
Vesicular trafficking					
AP-3 complex subunit delta	EHI_164810	116 kDa	0.00	5.05	NA
Vacuolar protein sorting 35	EHI_002990	87 kDa	0.00	5.05	NA
Beta prime-COP	EHI_004590	91 kDa	0.00	4.21	NA
Dynamin-like protein	EHI_052740	75 kDa	0.00	2.52	NA
Coatomer subunit beta	EHI_027720	95 kDa	0.00	2.52	NA
Vacuolar protein sorting 26	EHI_062490	48 kDa	0.00	2.52	NA
Beta2-COP (Fragment)	EHI_088220	104 kDa	1.23	4.21	3.41
Adaptor protein (AP) family protein	EHI_013040	123 kDa	2.47	5.89	2.39
Rab family GTPase	EHI_117960	21 kDa	1.23	2.52	2.05
EhSec23A	EHI_008730	81 kDa	1.23	2.52	2.05
EhSyntaxin B	EHI_021410	26 kDa	1.23	2.52	2.05

Figure 4. Identification of PI3P-binding effector proteins involved in phagosome biogenesis.
(a) The strategy and rationale used in this study to identify PI3P-binding effector proteins involved in phagosome biogenesis. See text for details.
(b) Expression of GFP-HrsFYVE under the tetracycline induction. Approximately 1×10^5 of trophozoites were cultivated with 10 μg/ml tetracycline for 0-48 hr, harvested, and subjected to SDS-PAGE and immunoblot analyses. Approximately 20 μg protein of lysates at each time point was electrophoresed. An arrowhead indicates GFP-HrsFYVE.
(c) Verification of the recruitment of GFP-HrsFYVE to phagosomes by fluorescent microscopy. The *E. histolytica* transformant cells that expressed GFP-HrsFYVE under tetracycline induction were cultured in the presence of 10 μg/ml of tetracycline for 24 h and then incubated with human serum coated beads for 30 min. Arrowheads indicate ingested beads.
(d) Validation of the recruitment of GFP-HrsFYVE to phagosomes by phagosome purification followed by immunoblot analysis. The beads-containing phagosomes were purified as described in 2-7-1 Phagosome purification and subjected to SDS-PAGE and immunoblot analyses. GFP-HrsFYVE and mature CP-A5 were detected with anti-myc, anti-GFP, and anti-CP-A5 antibody, respectively.
(e) The categorized list of proteins that are differentially excluded from phagosomes in GFP-HrsFYVE-dependent fashion. Tet(+) and tet(-) indicate the conditions where GFP-HrsFYVE expression was induced with 10 μg/ml of tetracycline or not induced. The values indicate the relative frequency of the detected peptides corresponding to each protein. "tet(-)/tet(+)" indicates the division of the value of tet(-) by the value of tet(+).

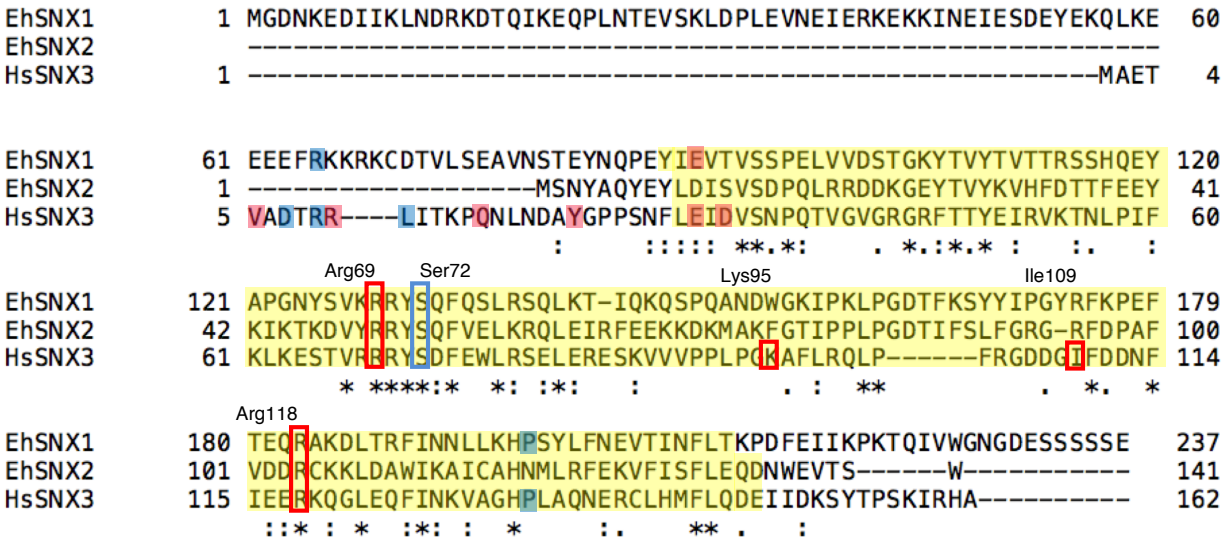

Figure 5. Alignment of protein sequences of EhSNX1, EhSNX2, and HsSNX3.
Protein sequences were aligned using clustalw algorithm (http://clustalw.ddbj.nig.ac.jp). PX domain sequences were predicted by HMMER (Meng and Ji, 2013) and are shown with yellow background. The numbers by three amino acid sequences (EhSNX1, EhSNX2, and HsSNX3) correspond to the amino acid positions of each protein, while those on top of the sequences (Arg69, Ser72, Lys95, Ile109, and Arg118) correspond to the amino acid positions of the residues in HsSNX3 (Lenoir et al., 2018). Ser72 was previously shown to be phosphorylated and marked with a blue rectangle, while the other residues implicated for PI3P binding are marked with red rectangles. Important residues for binding to Vps26 and Vps35 are shown with blue and pink highlight, respectively.

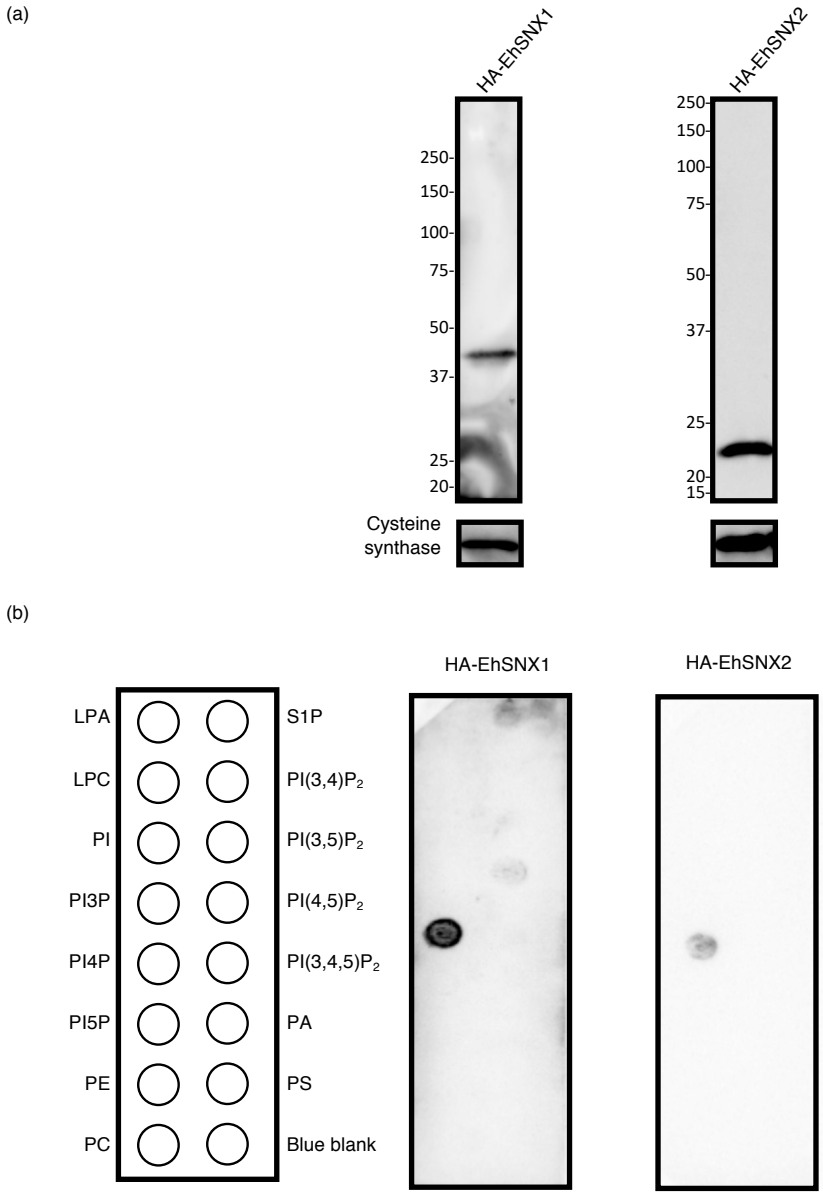

Figure 6. Lipid binding specificity of EhSNX1 and EhSNX2.
(a) Verification of the expression of EhSNX1 and EhSNX2 in HA-EhSNX1 and HA-EhSNX2 expressing transformants by immunoblotting using anti-HA antibody. Approximately 20 μg of total lysates from these strains were loaded. Cysteine synthase 1 was detected by anti-CS1 antiserum as a loading control.
(b) Lipid binding specificity of EhSNX1 and EhSNX2 observed by lipid overlay assay. A panel of PIPs and phospholipids spotted on nitrocellulose membrane was incubated with total lysates from HA-EhSNX1 and HA-EhSNX2 expressing transformants. The membranes were reacted with anti-HA antibody. Abbreviations are: LPA, lysophosphatidic acid; LPC, lysophosphocholine; PE, phosphatidylethanolamine; PC, phosphatidylcholine; S1P, sphingosine-1-phosphate; PA, phosphatidic acid; PS, phosphatidylserine.

(a)

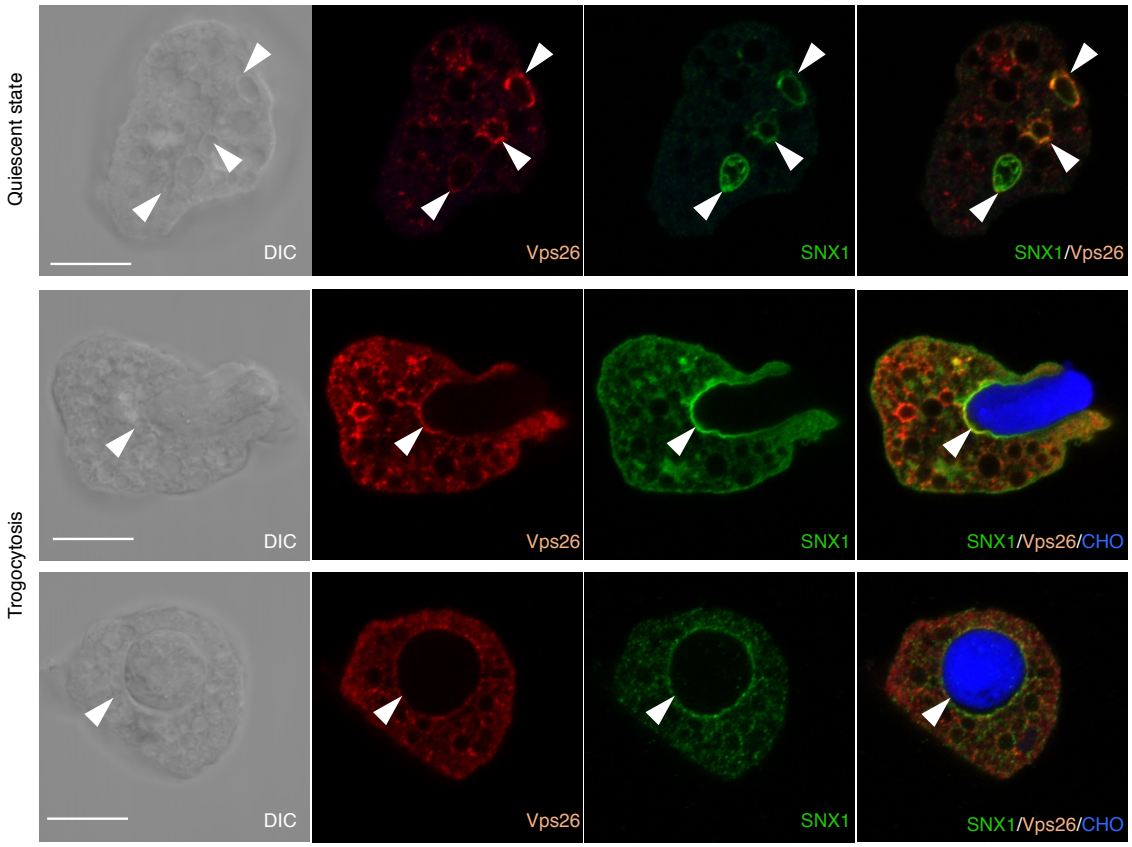
Quiescent state
Trogocytosis
DIC
Vps26
SNX1
SNX1/Vps26
DIC
Vps26
SNX1
SNX1/Vps26/CHO
DIC
Vps26
SNX1
SNX1/Vps26/CHO

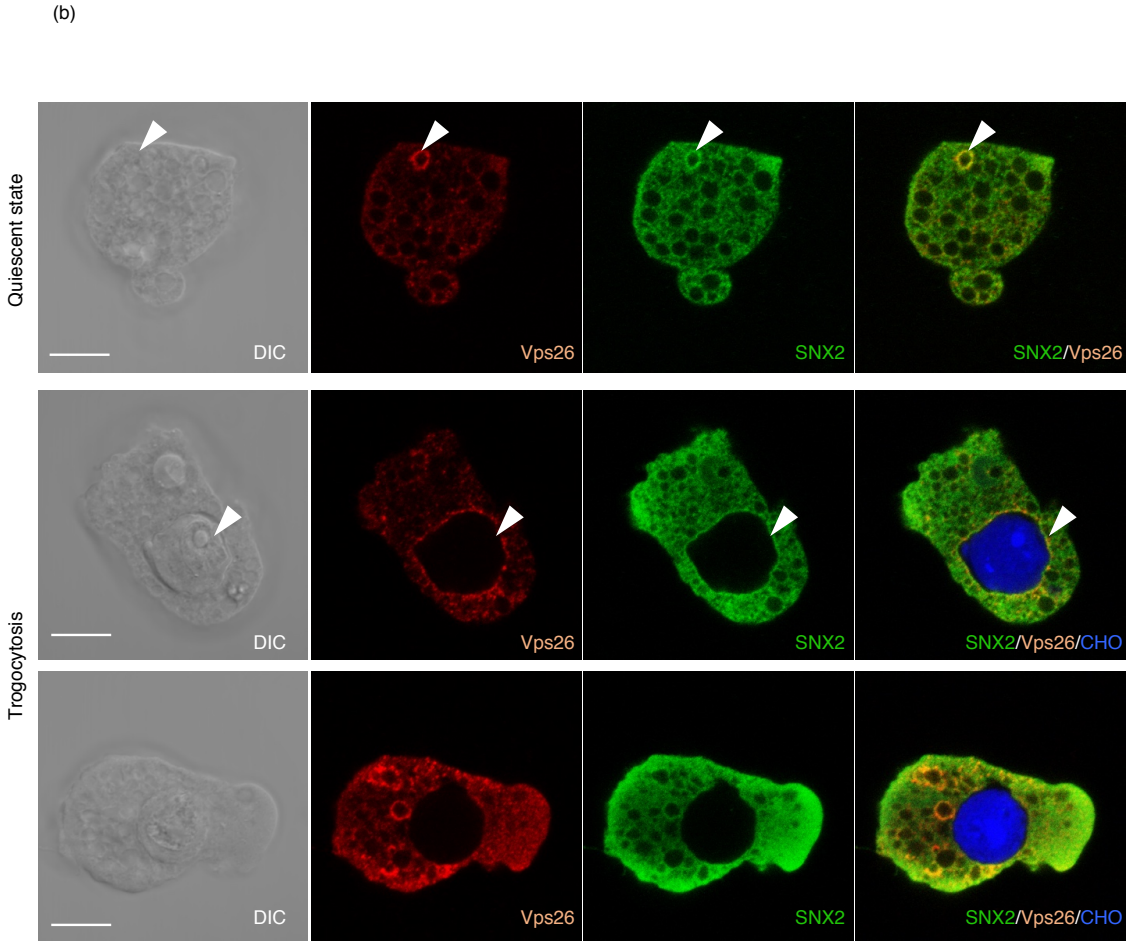

Figure 7. Localization of HA-EhSNX1 and HA-EhSNX2.
Localization of EhSNX1 and EhSNX2 (a, b) was examined by Immunoflorescence assay (IFA) in quiescent state and during phagocytosis. HA-EhSNX1/2 and EhVps26 were detected by anti-HA antibody and anti-EhVps26 antiserum, respectively. HA-EhSNX1/2 are shown in green, EhVps26 in red, and CHO cells were stained by CellTracker Blue. Differential interference contrast (DIC) and fluorescence images are shown. Scale bars are 10 μm. Upper panels, in quiescent state; middle panels, during internalization of a CHO cell (a), after closure of the trogosome (b); lower panels, after closure of the trogosome. Arrowheads depict vesicles, vacuoles, phagosomes, and the phagocytic cup where EhSNX1 or 2 is co-localized with EhVps26.

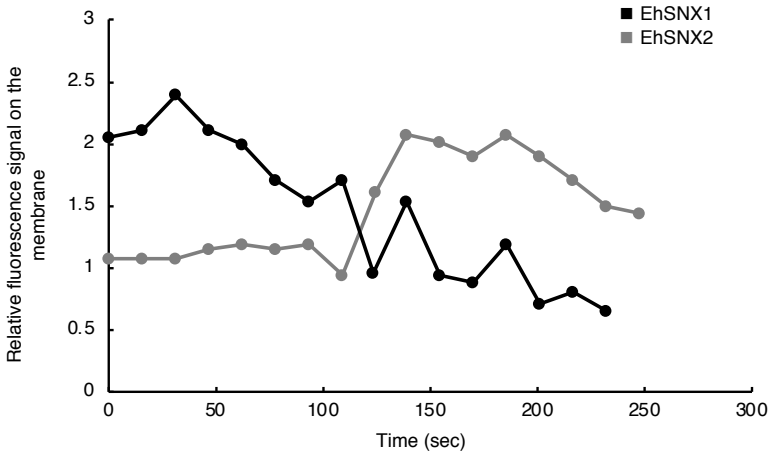

Figure 8. Kinetics of association of GFP-EhSNX1/2 to the trogosome membrane during CHO cell internalization.
Fluorescence intensity of GFP-EhSNX1/2 on the trogosome membrane relative to the cytoplasm was monitored during trogocytosis of CHO cells. The images started to be collected 4-7 sec after the initiation of the trogocytic cup formation, and this timing was set to zero. Y axis represents the mean fluorescence signal per pixel of GFP-SNX1/2 on the trogosome membrane relative to that in the cytosol. One representative image each of three independent experiments is shown. Only representative movies were analyzed, but other movies also showed similar kinetics.

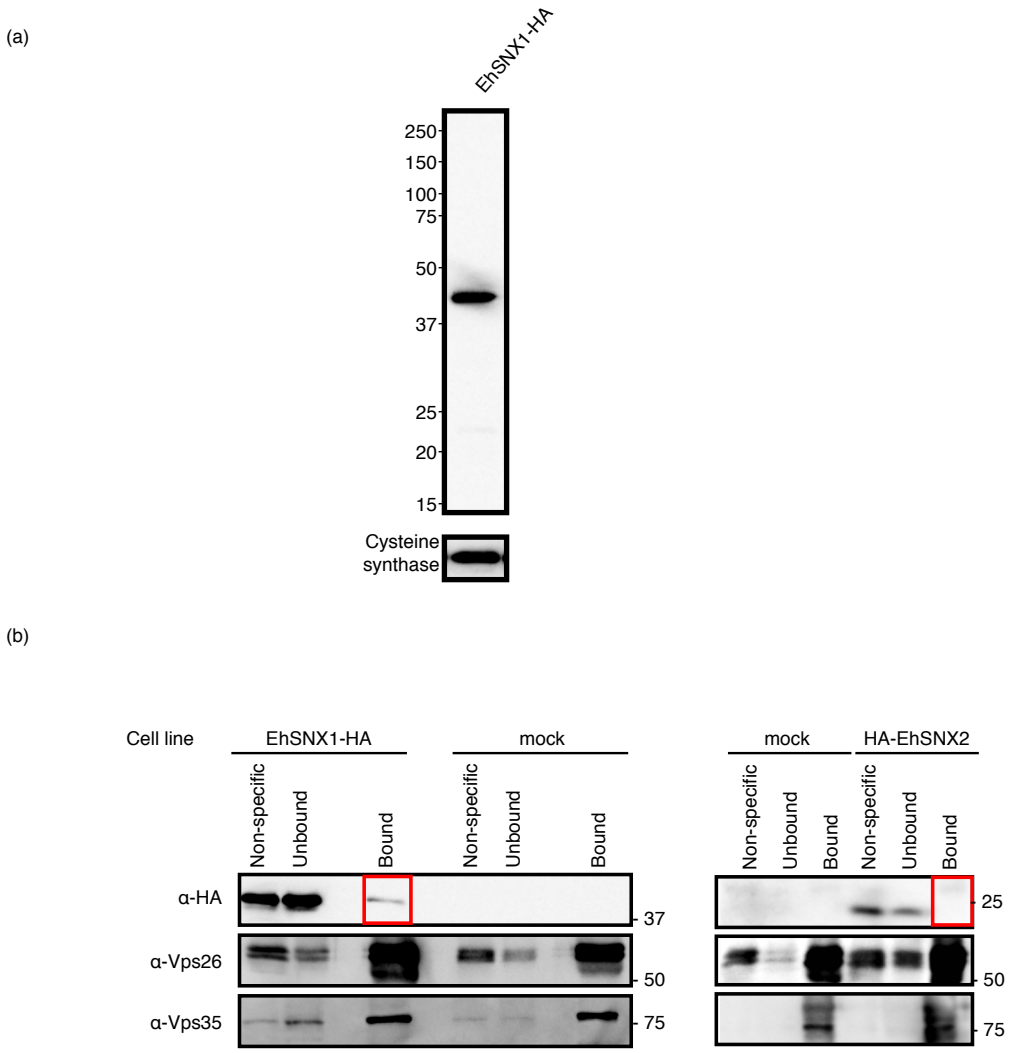

Figure 9. Binding of EhSNX1 with the retromer complex.
(a) Verification of the expression of EhSNX1-HA by immunoblot analysis using anti-HA antibody. Approximately 20 μg of total lysates from these strains were loaded. Cysteine synthase 1 was detected by anti-CS1 antiserum as a loading control.
(b) Immunoprecipitation of EhVps26 and EhSNX1-HA followed by immunoblot analysis. After 30 min co-culture with EhSNX1-HA, HA-EhSNX2, or mock transformant cells with CHO cells, the amoebae were collected to produce lysates, which were subjected to immunoprecipitation by anti-Vps26 antiserum. The immunoprecipitated ("Bound"), unbound supernatant ("Unbound"), and non-specific (Protein G-Sepharose control beads that were preincubated with lysates, washed, and boiled with SDS loading buffer) fractions were analyzed with SDS-PAGE and immunoblot analyses using anti-HA antibody, anti-Vps26, and anti-Vps35 antisera.

(a)

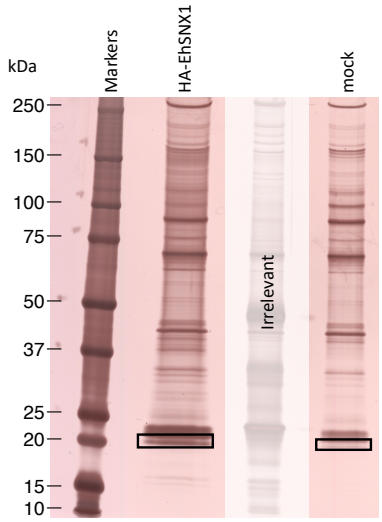

(b)

name of proteins	accession number	MW	HA	HA-SNX1	tet (-)/tet (+)
Actin-related protein 2/3 complex subunit 3	EHI_174910	22 kDa	0.00	2.73	NA
Uncharacterized protein	EHI_050520	25 kDa	0.00	1.36	NA
Putative uncharacterized prote	EHI_140760	23 kDa	0.79	2.73	3.45
Putative uncharacterized prote	EHI_169900	21 kDa	0.79	2.73	3.45
ARP2/3 complex 20 kDa subu	EHI_030820	22 kDa	0.79	1.36	1.73
Putative uncharacterized prote	EHI_155310	24 kDa	0.79	1.36	1.73
Putative uncharacterized prote	EHI_107790	22 kDa	1.58	1.36	0.86
Grainin 1	EHI_167300	24 kDa	6.32	1.36	0.22

(c)

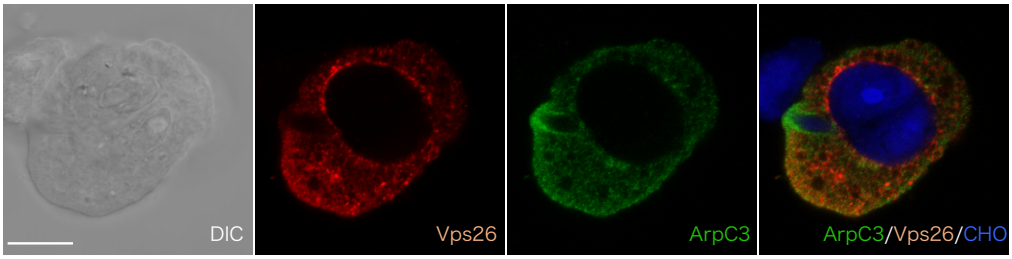

Figure 10. The identification of the binding protein of EhSNX1.
(a) The silver stained SDS-PAGE gel of the immunoprecipitated samples from HA-EhSNX1 and mock transformants using anti-HA antibody. The rectangles indicate the region of the specific band excised from HA-EhSNX1 and its corresponding region from control.
(b) The proteins that were detected from the unique band specifically recognized from HA-EhSNX1 expressing transformants by immunoprecipitation using anti-HA antibody. Proteins that were not detected from the HA-EhSNX1 are excluded from the table. The values indicate the relative frequency of the detected peptides corresponding to each protein. “HA-EhSNX1/HA” indicates the division of the value of HA-EHhSNX1 by the value of HA control. A whole list of the detected proteins is found in Supplementary Table 2.
(c) The localization of EhArpC3 and EhVps26 during trogocytosis. FLAG-EhArpC3 transformant was co-cultured with CHO cells stained with CellTracker Blue for 15 min. FLAG-EhArpC3 and EhVps26 were detected using anti-FLAG antibody and anti-EhVps26 antiserum. FLAG-EhArpC3 is shown in green, EhVps26 is shown in red. Scale bar is 10 μm.

(a)

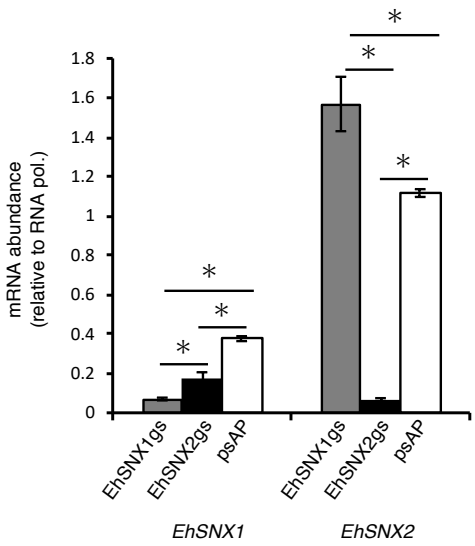
mRNA abundance
(relative to RNA pol.)
1.8
1.6
1.4
1.2
1
0.8
0.6
0.4
0.2
0
*
*
*
*
*
EhSNX1gs
EhSNX2gs
psAP
EhSNX1gs
EhSNX2gs
psAP
EhSNX1
EhSNX2

(b)

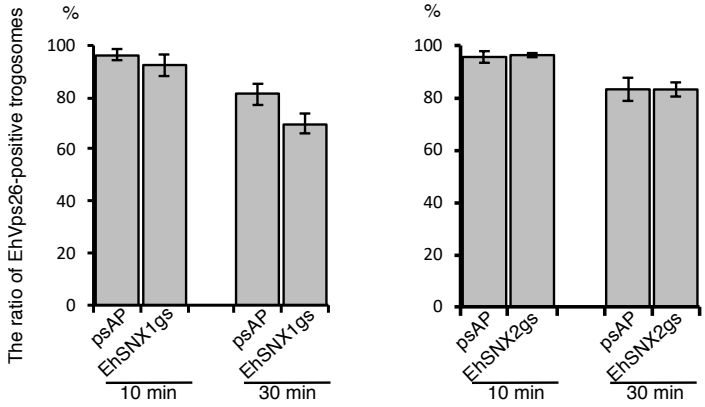
The ratio of EhVps26-positive trogosomes
%
100
80
60
40
20
0
psAP
EhSNX1gs
psAP
EhSNX1gs
10 min
30 min
%
100
80
60
40
20
0
psAP
EhSNX2gs
psAP
EhSNX2gs
10 min
30 min

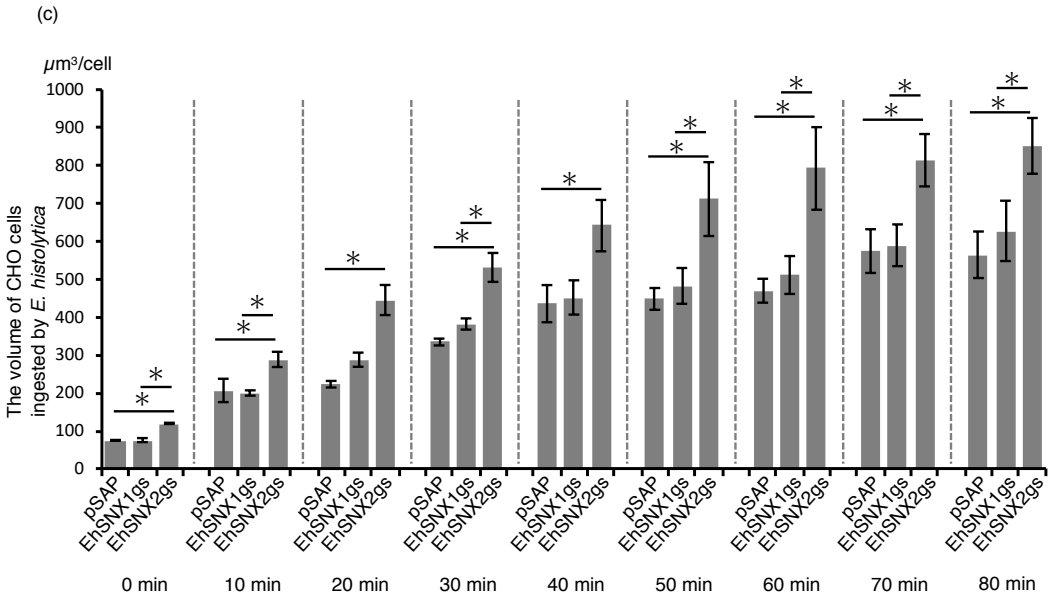

Figure 11. The effect of gene silencing of *EhSNX1* and *EhSNX2* on the retromer recruitment to trogosomes and trogocytosis.
(a) The levels of *EhSNX1* and *EhSNX2* transcripts in EhSNX1gs, EhSNX2gs, and control strains. The levels of the transcripts are shown relative to that of RNA polymerase II.
(b) The effects of gene silencing of *EhSNX1* and *EhSNX2* on the recruitment of EhVps26 to trogosomes. Trophozoites were allowed to ingest live CHO cells for 10 or 30 min, and subjected to IFA. Images of trophozoites that had ingested CHO cells were randomly captured, and the number of all trogosomes and Vps26-positive trogosomes were counted to estimate the ratio of Vps26-positive trogosomes.
(c) The effects of gene silencing of *EhSNX1* and *EhSNX2* genes on trogocytosis. Trophozoites of EhSNX1gs and EhSNX2gs strains stained with CellTracker Green were incubated with CHO cells stained with CellTracker Blue as described in Materials and Methods 2-1-14. The images were taken on CQ1 every 10 min for 80 min. The volume of the ingested CHO cells (blue) was calculate using three dimensionally reconstituted data. Bars indicate standard errors. Asterisks indicate statistical significance by Tukey-test ($p<0.05$). Experiments were conducted three times independently, and a representative data set is shown.

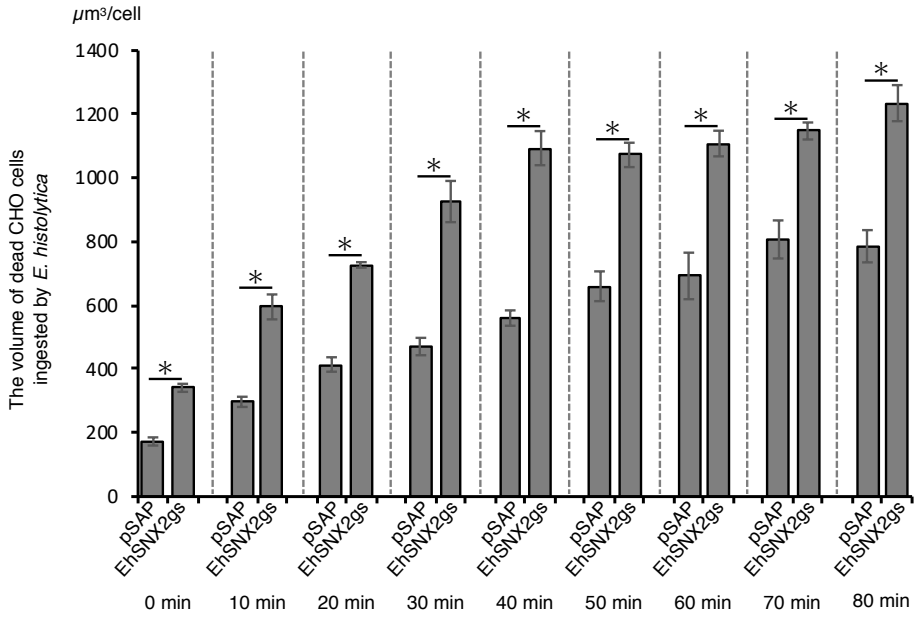

Figure 12. The effects of gene silencing of *EhSNX2* genes on phagocytosis of prekilled CHO cells.

Trophozoites of EhSNX2gs and control strains stained with CellTracker Green were incubated with prekilled CHO cells stained with CellTracker Blue. The images were taken on CQ1 every 10 min for 80 min. The volume of the ingested dead CHO cells (blue) was calculate using three dimensionally reconstituted data. Bars indicate standard errors. Asterisks indicate statistical significance by Tukey-test (p<0.05). Experiments were conducted three times independently, and a representative data set is shown.

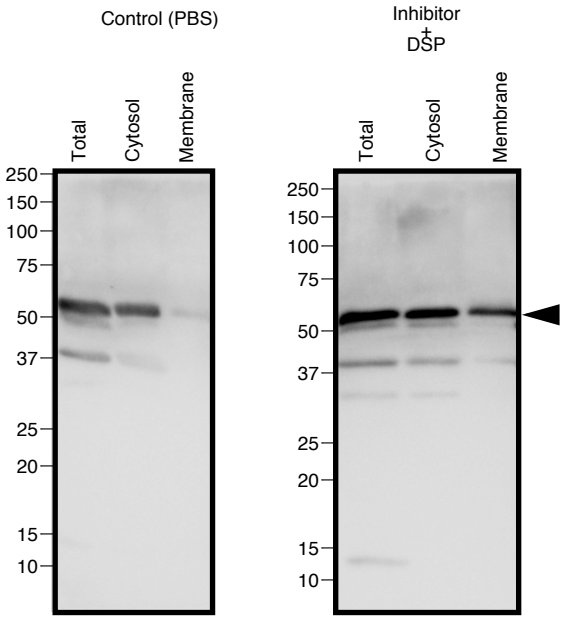

Figure 13. Effects of phosphatase inhibitors and cross linker on the stability of GFP-HrsFYVE. Approximately 1×10^7 of trophozoites were cultivated with 10 μg/ml tetracycline for 24 hr and harvested. Cells were treated or untreated with DSP, β-glycerophosphate, EDTA, sodium fluoride, and sodium orthovanadate. They were homogenized by a Dounce homogenizer and separated into cytosol and membrane fractions by centrifugation at 100,000 $\times$ g for 1 hr. The fractions were subjected to SDS-PAGE and immunoblot analyses stained with anti-GFP antibody. Approximately 20 μg protein of fractions was electrophoresed. An arrowhead indicates GFP-HrsFYVE.

```
HsSNX1  143 FDLTVGITDP EKIGDGMNAY VAYKVTTQTS LPLFRSKQFA VKRRFSDFLG LYEKLSEKHS Q------NGF 206
HsSNX2  140 FDIEIGVSDP EKVGDGMNAY MAYRVTTKTS LSMFSKSEFS VKRRFSDFLG LHSKLASKYL H------VGY 203
HsSNX3   29 --LEIDVSNP QTVGVGRGRF TTYEIRVKTN LPIFKLKEST VRRRYSDFEW LRSELERE-- -------SKV  87
EhSNX1   88 -YIEVTVSSP ELVVDSTGKY TVYTVTTRSS HQEYAPGNYS VKRRYSQFQS LRSQLKTI-Q KQSPQANDWG 155
EhSNX2   10 --LDISVSDP QLRRDDKGEY TVYKVHFDTT FEEYKIKTKD VYRRYSQFVE LKRQLEIRFE EKKDKMAKFG  77

HsSNX1  207 IVPPPPEKSL IGMTKVKVGK EDSSSAEFLE KRRAALERYL QRIVNHPTML QDPDVREFLE KE 268
HsSNX2  204 IVPPAPEKSI VGMTKVKVGK EDSSSTEFVE KRRAALERYL QRTVKHPTLL QDPDLRQFLE SS 265
HsSNX3   88 VVPPLPGKAF LRQLPF-RGD DGIFDDNFIE ERKQGLEQFI NKVAGHPLAQ NERCLHMFLQ DE 148
EhSNX1  156 KIPKLPGDTF KSY----YIP GYRFKPEFTE QRAKDLTRFI NNLLKHPSYL FNEVTINFLT -- 211
EhSNX2   78 TIPPLPGDTI FSL----FGR G-RFDPAFVD DRCKKLDAWI KAICAHNMLR FEKVFISFLE QD 134
```

Figure 14. Amino acid alignment of the PX domain of HsSNX1-3 and EhSNX1-2.
The residues conserved in EhSNX1-2 and HsSNX3, but not in HsSNX1-2, are shown with yellow background. Corresponding numbers denote position of amino acid residue based on respective amino acid sequences.

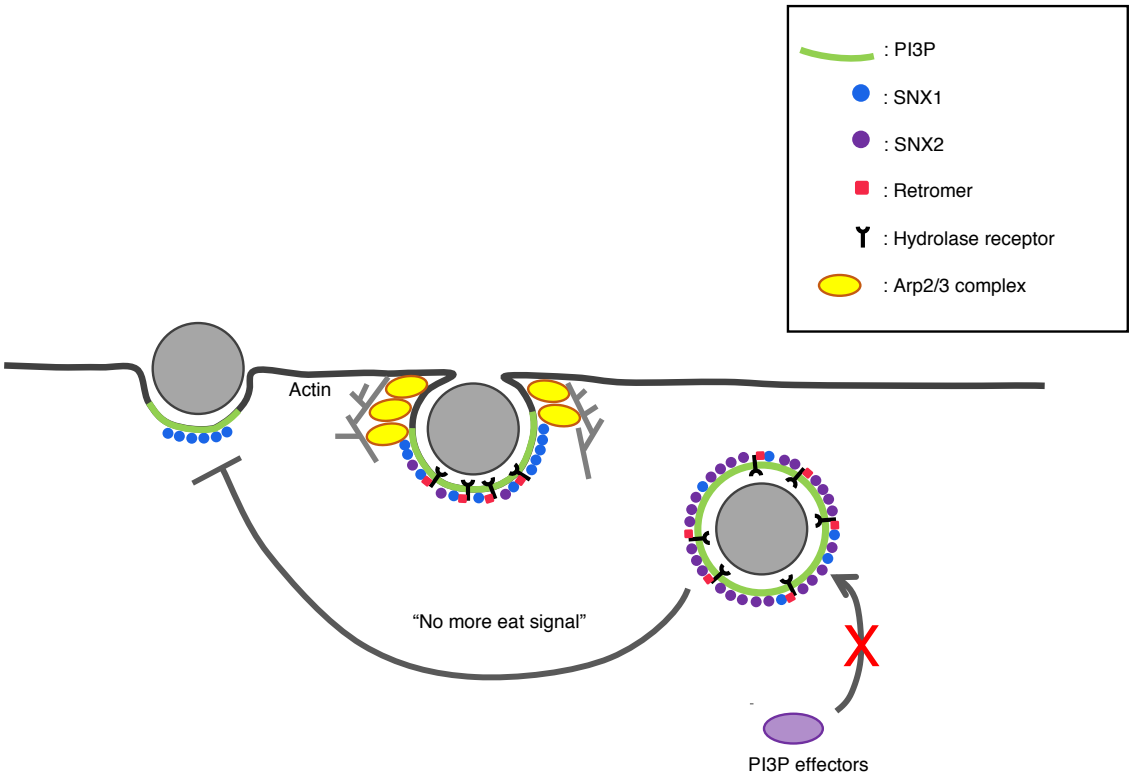

Figure 15. A model of the involvement of PI3P, SNXs, the retromer, the hydrolase receptor, and Arp2/3 complex in amoebic phago/trogocytosis.

Enzyme		Query: Protein name (*H. sapiens*)	Query: Gene name (*H. sapiens*)	Accession No.	NLS	Homologue in *E. histolytica*: Amoeba gene ID No.	E-value	NLS
PI 3-kinase	Class I	p110α	PIK3CA	NP_006209		EHI_006130	4.00E-131	
		p110β	PIK3CB	NP_006210		EHI_095130	2.00E-115	
		p110γ	PIK3CG	AAH35683		EHI_040690	3.00E-105	
		p110δ	PIK3CD	NP_005017		EHI_013980	7.00E-103	
						EHI_188970	2.00E-103	
						EHI_009890	2.00E-57	
	Class II	PIK3C2α	PIK3C2A	NP_002636				
		PIK3C2β	PIK3C2B	NP_002637				
		PIK3C2γ	PIK3C2G	NP_001275701				
	Class III	Vps34	PIK3C3	AAH53651		EHI_096560	1.00E-87	

Table1. Potential PI 3-kinase orthologues in *E. histolytica*. *H. sapiens* enzymes use as queries, and E-value are shown.

	Query				Homologue in *E. histolytica*		
	Protein name (*H. sapiens*)	Gene name (*H. sapiens*)	Accession No.	NLS	Amoeba gene ID No	E-value	NLS
PI 3-phosphatase	PTEN	PTEN	AAD13528	10-19	EHI_197010	3.00E-64	
					EHI_098450	3.00E-57	
					EHI_131070	3.00E-52	
					EHI_041900	7.00E-44	152-167, 153-164
					EHI_010360	1.00E-39	
					EHI_054460	7.00E-31	
	TPIPα	TPIPα	CAD13144.1				
	TPIPβ	TPIPβ	CAD13145.1				
	TPIPγ	TPIPγ	AAP 45146.1				
	MTM1	MTM1	NP_000243		EHI_070120	1.00E-92	18-49
	MTMR3	MTMR3	AAI52456.1		EHI_161190	8.00E-89	
	MTMR6	MTMR6	EAX08367.1		EHI_049780	2.00E-82	
	MTMR9	MTMR9	NP_056273.2		EHI_016430	3.00E-78	
					EHI_031310	7.00E-75	
					EHI_104710	7.00E-64	
					EHI_024380	2.00E-64	
					EHI_188050	3.00E-59	
					EHI_087780	2.00E-58	
					EHI_140980	7.00E-64	
	MTMR14	MTMR14	AAH01674.2				
	MTMR5	MTMR5	NP_002963.2				
	inactive myotubularin/LRR/ROCO/kinase (IMLRK)				EHI_137960	1.00E-15	
					EHI_135010	3.00E-10	
					EHI_151670	2.00E-05	
					EHI_048230	1.00E-04	
					EHI_078170	4.00E-04	
					EHI_185230	1.00E-03	
					EHI_197200	1.00E-03	
					EHI_141820	2.00E-03	
					EHI_107230	6.60E-02	

Table2. Potential PI 3-phosphatases orthologues in *E. histolytica*. *H. sapiens* enzymes use as queries, and E-value are shown.